CPTR 72
MARCH 2001

SUBSCALE FAST COOKOFF TESTING AND MODELING FOR THE HAZARD ASSESSMENT OF LARGE ROCKET MOTORS

J. E. Cocchiaro

CHEMICAL PROPULSION INFORMATION AGENCY

• THE JOHNS HOPKINS UNIVERSITY •
• WHITING SCHOOL OF ENGINEERING • COLUMBIA, MARYLAND 21044-3200 •

REPORT DOCUMENTATION PAGE

Form Approved
OMB No. 0704-0188

AGENCY USE ONLY *(Leave Blank)*	REPORT DATE	REPORT TYPE AND DATES COVERED
	March 2001	Technical Report, 1965 to 2001

4. TITLE AND SUBTITLE

Subscale Fast Cookoff Testing and Modeling for the Hazard Assessment of Large Rocket Motors

5. FUNDING NUMBERS

SP0700-97-D-4004

6. AUTHOR(S)

Cocchiaro, J. E.

7. PERFORMING ORGANIZATION NAME(S) AND ADDRESS(ES)

The Johns Hopkins University
Chemical Propulsion Information Agency
10630 Little Patuxent Parkway, Suite 202
Columbia, MD 21044-3204

8. PERFORMING ORGANIZATION REPORT NUMBER

CPTR 72

9. SPONSORING/MONITORING AGENCY NAME (S) AND ADDRESS(ES)

DTIC - AI
8725 John J. Kingman Road
Suite 0944
Ft. Belvoir, VA 22060-6218

Naval Air Warfare Center Weapons Division
Code 477000D
China Lake, CA 93555-6100

10. SPONSORING/MONITORING AGENCY REPORT NUMBER

11. SUPPLEMENTARY NOTES

Hardcopies available from CPIA only. CPIA's DTIC-assigned source code is 423900.

12a. DISTRIBUTION/AVAILABILITY STATEMENT

Approved for public release; distribution is unlimited

12b. DISTRIBUTION CODE

13. ABSTRACT *(Maximum 200 words)*

A significant issue facing the solid propulsion acquisition and safety communities is to determine if hazard classification requirements can be structured for large solid rocket motor programs to maximize safety while optimizing the tradeoff between safety and logistical considerations and system acquisition costs. Integral to this assessment is an evaluation of the potential application of subscale analog testing and modeling to characterize the full-scale motor response in a variety of scenarios such as in an engulfing fuel fire (fast cookoff) or wood bonfire environment. This information is necessary for final hazard classification and insensitive munitions (IM) assessment purposes for new systems.

This report summarizes fast cookoff testing diagnostic techniques, subscale analog hazard response tests, established computer modeling analysis techniques, and other empirical information that might be useful for scaling the results of a subscale analog fast cookoff/bonfire test to a full-size solid rocket motor (SRM) for hazard classification and/or IM assessment. Since subjective observations and judgment cannot be completely eliminated from a subscale test protocol, an integral aspect of the scaling issue makes use of empirical (experimental) motor hazard response information that has been gained from full-scale fast cookoff/bonfire tests and related, well characterized accidents exhibiting similar failure modes. Thus, the final part of the report summarizes findings of fast cookoff parametric test programs and other miscellaneous full-scale test results with solid rocket motors containing high-energy propellants.

14. SUBJECT TERMS

Environmental tests
Fire hazards
Hazards
Model tests
Safety
Scale models
Solid propellant rocket engines
Test and evaluation
Test methods
Vulnerability

15. NUMBER OF PAGES

60

16. PRICE CODE

17. SECURITY CLASSIFICATION OF REPORT	18. SECURITY CLASSIFICATION OF THIS PAGE	19. SECURITY CLASSIFICATION OF ABSTRACT	20. LIMITATION OF ABSTRACT
UNCLASSIFIED	UNCLASSIFIED	UNCLASSIFIED	UA

CPTR 72
MARCH 2001

SUBSCALE FAST COOKOFF TESTING AND MODELING FOR THE HAZARD ASSESSMENT OF LARGE ROCKET MOTORS

J. E. Cocchiaro

CHEMICAL PROPULSION INFORMATION AGENCY

• THE JOHNS HOPKINS UNIVERSITY •
• WHITING SCHOOL OF ENGINEERING • COLUMBIA, MARYLAND 21044-3200 •

The Chemical Propulsion Information Agency (CPIA) is a DoD Information Analysis Center Operated by The Johns Hopkins University, Whiting School of Engineering, under Defense Supply Center Columbus (DSCC) contract SPO700-97-D-4004. The applicable DoD Instruction is 3200.12-R-2, "Centers for Analysis of Scientific and Technical Information" The CPIA's mailing address is The Johns Hopkins University, Chemical Propulsion Information agency, Attention: Security Office, 10630 Little Patuxent Parkway, Suite 202, Columbia, Maryland 21044-3204.

The CPIA also provides technical and administrative support to the Joint Army-Navy-NASA-Air Force (JANNAF) Interagency Propulsion Committee.

The Government Administrative Manager for CPIA is the Defense Technical Information Center, Code DTIC-AI, 8725 John J. Kingman Road, Suite 0944, Ft. Belvoir, Virginia 22060-6218. The Government Technical Manager (Contracting Officer's Technical Representative) is Mr. Stuart R. Blashill, Naval Air Warfare Center Weapons Division, Code 477000D, China Lake, California 93555-6001.

PREFACE

This issue of the Chemical Propulsion Technology Reviews (CPTR 72) continues CPIA's recurrent series of technical summaries and status reports on topics pertaining to missile, space, and gun propulsion technology.

This study was conducted in support of current activities being undertaken by the Department of Defense Explosives Safety Board (DDESB), Alexandria, Virginia, and the Joint Army-Navy-NASA-Air Force (JANNAF) Propulsion Systems Hazards Subcommittee (PSHS) to examine the feasibility of establishing an alternate subscale test/modeling hazard classification protocol appropriate for large rocket motor systems. Partial funding for this work was provided by the DDESB.

The general aim of this study is to collect, analyze, and summarize information from past RDT&E efforts related to the assessment of the hazard response of a rocket motor in an engulfing fuel or wood fire environment. Full-scale motor response in this scenario is of significant interest in determining the appropriate final hazard classification as well as insensitive munitions (IM) characteristics of a rocket motor; however, destructive testing with full-scale solid rocket motor assets is undesirable to an acquisition program for many reasons. The purpose of this report is to establish a baseline from which the propulsion, safety, and IM communities can consider in evaluating subscale bonfire testing as a hazard assessment approach, and/or identifying appropriate research priorities necessary to validate an acceptable subscale hazard assessment protocol for large rocket motors.

Comments or questions on the CPTR effort, including suggestions on topics for future issues, can be communicated to CPIA by using the enclosed response sheet, or by writing or calling Mr. James Cocchiaro, at (410) 992-9950 ext. 208, or by email at: jecocch@jhu.edu. Individuals employed by organizations that subscribe to CPIA services may request personal copies of this document by contacting CPIA at (410) 992-7300; email cpia@jhu.edu; website http://www.cpia.jhu.edu/.

ABSTRACT

A significant issue facing the solid propulsion acquisition and safety communities is to determine if hazard classification requirements can be structured for large solid rocket motor programs to maximize safety while optimizing the tradeoff between safety and logistical considerations and system acquisition costs. Integral to this assessment is an evaluation of the potential application of subscale analog testing and modeling to characterize the full-scale motor response in a variety of scenarios such as in an engulfing fuel fire (fast cookoff) or wood bonfire environment. This information is necessary for final hazard classification and insensitive munitions (IM) assessment purposes according to requirements as specified in policy documents "Department of Defense Ammunition and Explosives Hazard Classification Procedures," TB 700-2/NAVSEAINST 8020.8B/TO 11A-1-47/DLAR 8220.1, and "Hazard Assessment Tests for Non-Nuclear Munitions," MIL-STD 2105B (and the corresponding NATO guidance documents).

This report summarizes fast cookoff testing diagnostic techniques, subscale analog hazard response tests, established computer modeling analysis techniques, and other empirical information that might be useful for scaling the results of a subscale analog fast cookoff/bonfire test to a full-size solid rocket motor (SRM) for hazard classification and/or IM assessment. Since subjective observations and judgment cannot be completely eliminated from a subscale test protocol, an integral aspect of the scaling issue makes use of empirical (experimental) motor hazard response information that has been gained from full-scale fast cookoff/bonfire tests and related, well characterized accidents exhibiting similar failure modes. The possible correlation between propellant properties and motor system hazards, especially for high-energy (small critical diameter) propellants that may be more susceptible to detonation is of particular interest. Thus, the final part of the report summarizes findings of fast cookoff parametric test programs and other miscellaneous full-scale test results with solid rocket motors containing high-energy propellants.

CONTENTS

LIST OF FIGURES

LIST OF FIGURES (continued)

LIST OF FIGURES (continued)

LIST OF TABLES

GLOSSARY

1-D	One-dimensional
2-D	Two-dimensional
ALE3D	Arbitrary-Lagrange-Eulerian (3-D) Computer Code
ALEGRA	3-D Arbitrary-Lagrange-Eulerian Computer Code for Strong Shock Wave Solid Mechanics
AP	Ammonium Perchlorate
AUR	all-up round
CAE	Computer Aided Engineering
CALE	C-language Arbitrary Lagrangian-Eulerian (2-D) Computer Code
COYOTE	Nonlinear (2-3D) Finite Element Computer Code for Heat Transfer/Chemical Reaction Analysis
CTH	Nonlinear (2-3D) Computer Code for Large Deformation, Strong Shock Wave Solid Mechanics
DDT	Deflagration-to-Detonation Transition
DSC	Differential Scanning Calorimetry
DTA	Differential Thermal Analysis
DYNA2D	Nonlinear, Explicit, Two-dimensional Finite Element Computer Code for Solid Mechanics
ESD	Electrostatic Discharge
HARM	High Velocity Anti-radiation Missile
HONDO	Finite Element Computer Code for Axisymmetric, Large Deformation Solid Mechanics
HTPB	Hydroxy-terminated Polybutadiene
IM	Insensitive Munitions
IMAD	Insensitive Munitions Advanced Development
JAS3D	Nonlinear (3-D) Finite Element Computer Code for Quasistatic, Large Deformation Solid Mechanics
MSC	MSC Software Corporation
NASTRAN	General Purpose Finite Element Computer Code for Structural and Heat Transfer Analysis
NEPE	Nitrate Ester Polyether
NIKE2D	Nonlinear, Implicit, Two-dimensional Finite Element Computer Code for Solid Mechanics
PBX	Plastic Bonded Explosive
PERMS	Propellant Energetic Response to Mechanical Stimuli
RDT&E	Research, Development, Test, and Evaluation
SINDA	System Improved Numerical Differencing Analyzer Computer Code
SLBM	Submarine Launched Ballistic Missile
SPHT2D	Smooth Particle Hydrodynamics/Thermal (2-D) Computer Code
SRM	Solid Rocket Motor
TGA	Thermogravimetric Analysis
TOPAZ	Implicit Finite Element Computer Code for Heat Transfer/Chemical Reaction Analysis

1.0 INTRODUCTION

In recent years, there has been significant interest among Department of Defense acquisition programs to reduce costs associated with development and fielding of new munitions. Achieving system safety goals with reduced test and evaluation resources poses a significant challenge, and thus requires that innovative testing protocols be developed and validated. Historically, full-scale development hardware assets have been required for hazard classification and insensitive munitions (IM) assessment. A subscale hazard testing program in conjunction with modeling analysis offers the possibility of significant cost savings if the appropriate information can be determined. Subscale hazard testing and modeling may also improve confidence in limited full-scale test results performed on a statistically insignificant number of production items.

This report summarizes fast cookoff testing diagnostic techniques, subscale analog hazard response tests, established computer modeling analysis techniques, and other empirical information that might be useful for scaling the results of a subscale analog fast cookoff/bonfire test to a full-size solid rocket motor (SRM) for hazard classification and/or IM assessment. Full-scale motor response in an engulfing fuel fire (fast cookoff) or wood bonfire environment is of particular interest in determining the appropriate final hazard classification of a rocket motor. Since subjective observations and judgment cannot be completely eliminated from a subscale test protocol, an integral aspect of the scaling issue makes use of empirical (experimental) motor hazard response information that has been gained from full scale fast cookoff/bonfire tests and related, well characterized accidents exhibiting similar failure modes. The possible correlation between propellant properties and motor system hazards, especially for high energy (small critical diameter) propellants that may be more susceptible to detonation is of particular interest. Thus, the final part of the report summarizes findings of fast cookoff parametric test programs and other miscellaneous full-scale test results with solid rocket motors containing high energy propellants.

The report does not address one important aspect of the problem; that is, variability of the external source fire and possible effects of external variables on heat conduction into the system. Rather, the focus is on internal phenomenology associated with failure modes thought to influence the hazard response of a rocket motor, assuming simple heat conduction through the motor case wall.

2.0 THERMAL AND PHYSICAL RESPONSE OF THE MOTOR CASE AND LINER

2.1 Full-scale and Analog Motor Fast Cookoff Test Diagnostics

Significant research and development was conducted in the mid 1970's to early 1980's on possible mechanisms and corresponding physical/structural models detailing the response of a rocket motor in the fast cookoff scenario. Figure 1 illustrates a failure hypothesis developed through small-scale and well-instrumented full-scale tests, supporting analysis of Vetter[1] of the Naval Weapons Center, China Lake, CA, and small-scale and analog tests by Clark et al[2,3] of

Thiokol. Leining et al[4] of Hercules, Inc. also adopted this mechanism as the most credible during a joint Navy-Air Force program.

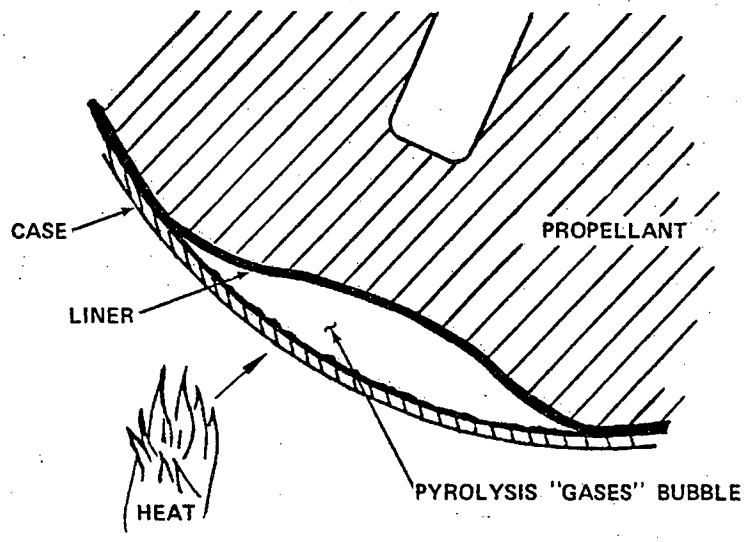

Figure 1. Physical Response of Rocket Motor During Initial Stage of Fast Cookoff[1]

The fast heating environment creates a high radial thermal gradient from the outside metal motor case wall towards the center bore of the propellant grain. Thermal decomposition (pyrolysis) and outgassing of the inside motor case primer and liner/insulation materials, in conjunction with possible thermal expansion of the motor case, produces a case to liner debond and subsequent pressurized gap between the liner/insulation and motor case before significant heating of the propellant occurs. The gas filled debond area may reduce heat transfer from the motor case to the motor interior, depending on whether or not the liner formulation produces clean gas, semi-solid, or other charred residue upon pyrolysis, causing a hot spot to develop on the motor case. As time progresses, gas pressure from liner pyrolysis or propellant combustion (if ignition has occurred at the outer propellant grain surface) may rupture the motor case at the hot spot and vent the system, or the pressure in the gap may cause collapse of the inner bore, structural failure (fracture) of the propellant grain, or unzipping of the case-liner bond. Venting of the case results in ambient pressure burning of the propellant grain from the outer surface towards the center bore. The latter two scenarios, on the other hand, might allow hot pyrolysis or combustion gases to ignite interior portions of the propellant grain resulting in confined deflagration of a significant propellant quantity at elevated pressure. The overall violence of the motor response will likely depend on the amount of propellant surface area involved in the deflagration (particularly if the grain becomes highly fractured), and the confinement provided to the burning propellant bed by the motor case. The ultimate dynamic pressurization will thus depend on the combined effects of many competing factors and processes associated with the motor case material, propellant-liner/insulation pyrolysis, propellant decomposition and ignitability, propellant and propellant-liner bond mechanical properties, etc. Pressure vessel type rupture/explosion of the motor case could be one outcome. In addition, it is at this point that deflagration-to-detonation transition needs to be considered, and the propellant critical diameter could perhaps influence the final system response.

The fundamental mechanism occurring under rocket motor fast heating has been verified from a variety of full-scale and analog motor tests using various diagnostic techniques. Thermocouple and pressure transducer measurements have been obtained at case-liner bond areas and in the grain inner bore to explore the pre-ignition and ignition phases, as well as burning evolution in rocket motor fast cookoff. Clark et al[2,3] obtained evidence of case-liner debond and air gap formation from thermocouple measurements with composite case analog motors containing high energy composite propellant (Fig. 2a). Figure 2b shows the transient loss of heat conduction into the inner surface of the propellant-liner (TC traces 18, 21, and 22) between 165 and 175 seconds due to case-liner air gap formation. This was followed by an abrupt rise in temperature at about 175 seconds indicating ignition at the outer propellant grain surface.

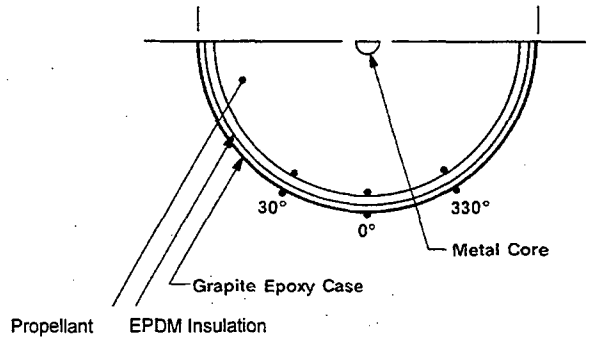

Thermocouple Numbering (End A to End B)			
Position	Outside Case	Inside Insulation	Core Surface
0°	1 - 3	10 - 14	25 - 26
30°	4 - 6	15 - 19	-------
330°	7 - 9	20 - 24	-------

NOTES:

1. Both ends closed
2. Inside thermocouples 2.0 inches apart

Figure 2a. Analog Motor Cross Section [3]

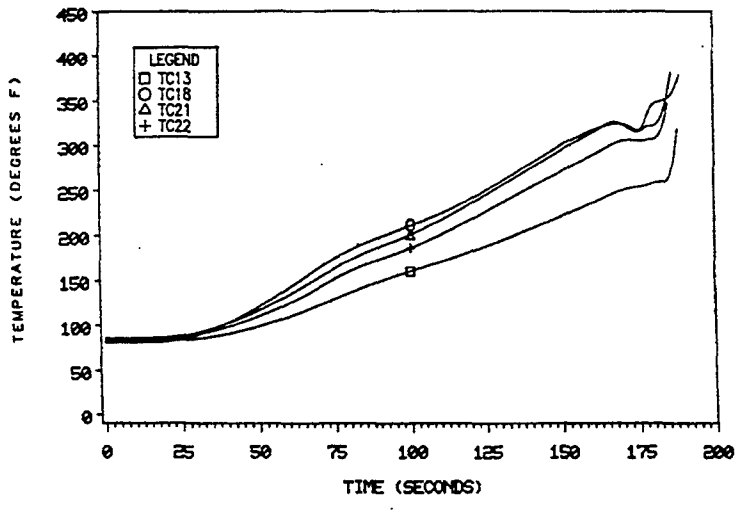

Figure 2b. Internal Liner Temperature During Fast Cookoff [3]

Further evidence was provided in full-scale fast cookoff tests with a generic Shrike motor configuration (Fig. 3) containing reduced smoke propellant[5]. Figure 4a shows the inner bore temperature trace (forward end) recorded in a representative test. Ignition occurred at the outside diameter of the propellant grain and the case subsequently vented 56 seconds into the test (as indicated from external video/sound coverage). The bore temperature trace indicates that the inner propellant bore did not ignite until approximately 67 seconds (from inverse burn-back of the propellant web). Between 30 and 48 seconds, a transient temperature rise in the propellant bore prior to ignition was also observed. The transient temperature increase was apparently not enough to cause ignition in the propellant bore, possibly due to the relatively low ignitability of the particular propellant[5]. Figure 4b shows a pressure spike at 67 seconds in the inner bore pressure trace, in agreement with the temperature measurements.

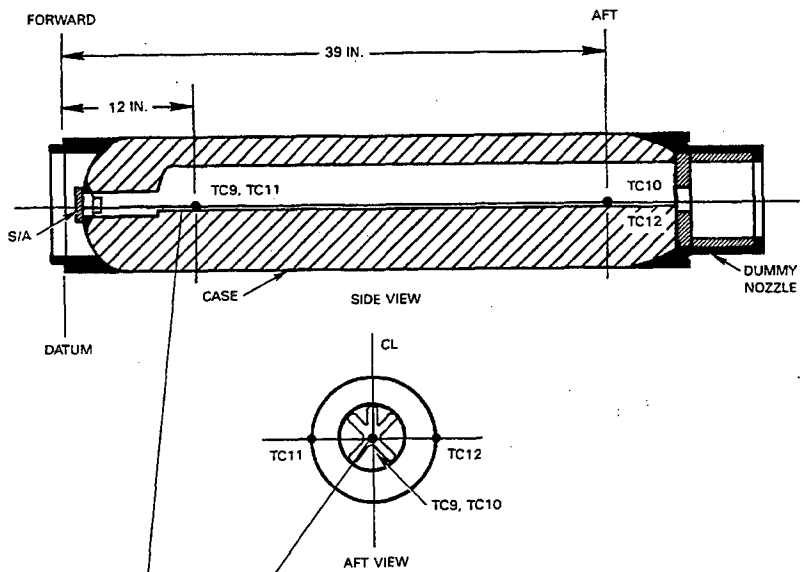

Figure 3. Instrumented Generic Shrike Rocket Motor Configuration Used in Fast Cookoff Tests [5]

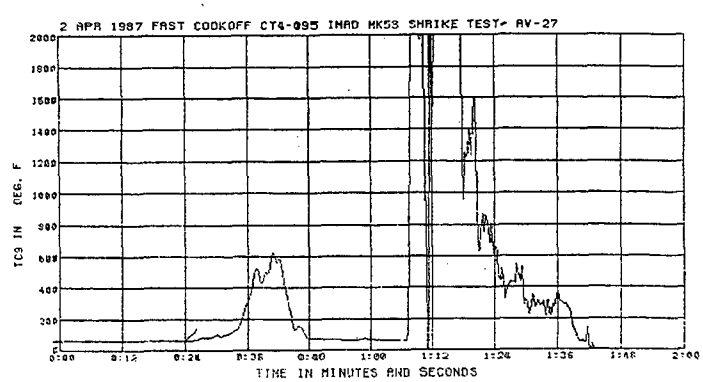

Figure 4a. Inner Bore Temperature Trace During Motor Fast Cookoff [5]

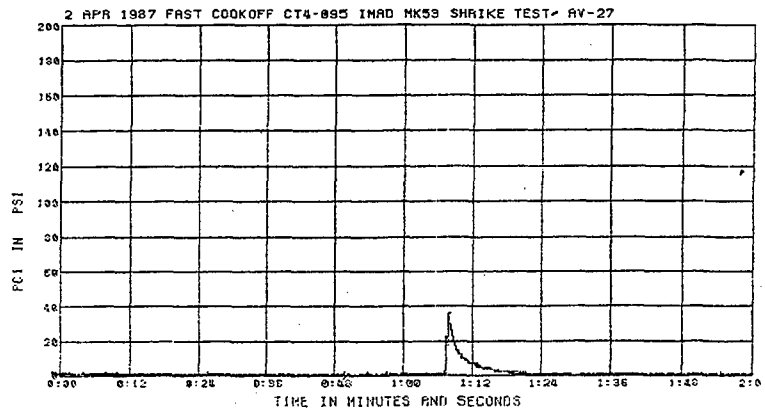

Figure 4b. Inner Bore Pressure Trace During Motor Fast Cookoff [5]

Similar results were obtained in a fast cookoff test of a generic Sidewinder motor (Fig. 5a) with reduced smoke propellant[1]. Figure 5b shows that ignition and initial burning occurred at the outside diameter of the propellant grain along the case-liner bond area, as indicated by the sharp increases of Thermocouples 2 and 5 up to propellant flame temperatures. Flame propagation to the propellant inner bore did not occur until a later time, as indicated by Thermocouples 6 and 7. Furthermore, flame propagation into the bore started at the aft (nozzle) end, since the aft thermocouple responded before the forward bore thermocouple. Due to the sequence of reaction propagation in both of these tests (first reaction at the outer grain diameter), the overall motor hazard response was fairly benign. Conversely, a test of a different generic Sidewinder configuration[1] showed near instantaneous flame propagation from the outer grain diameter near the aft end to the propellant inner bore surface (Fig. 6) due to bondline failure; the result was a more violent explosion of the motor. Artificial differences in the aft end insulation bondline and closure assembly (not representative of the Sidewinder flight hardware configuration) were thought to have influenced the result with this particular test item. In addition, poor propellant properties (high void content and inadequate mechanical properties) due to casting difficulties were also believed to promote a more violent reaction. The investigators concluded that, although the sample was inferior, the test served to demonstrate the importance of several motor parameters on fast cookoff response.

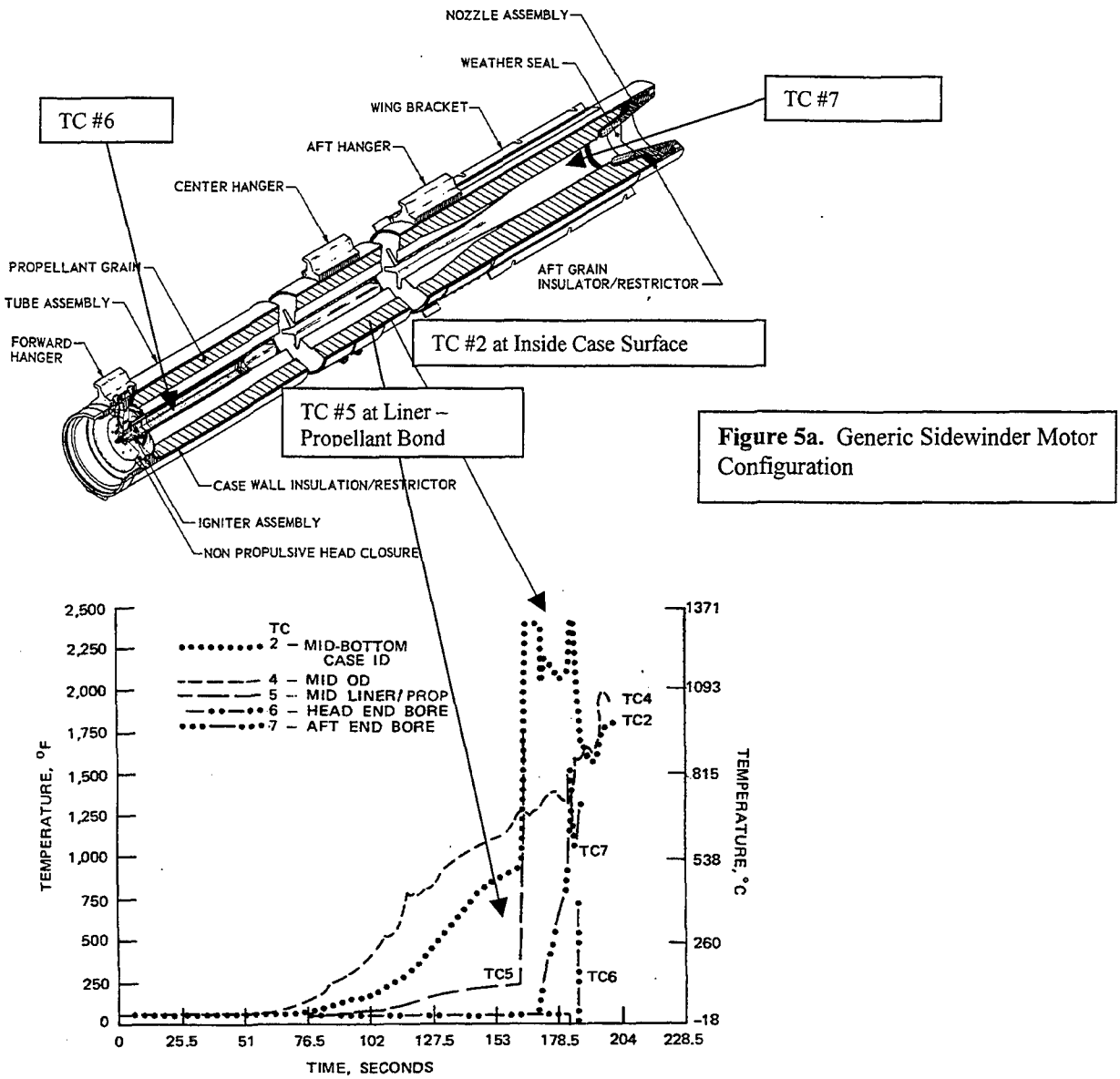

Figure 5a. Generic Sidewinder Motor Configuration

Figure 5b. Initial Temperature Spikes at Inside Case Wall and Inner Liner/Propellant Surface Show Ignition Occurred at Outside Propellant Grain Diameter[1]

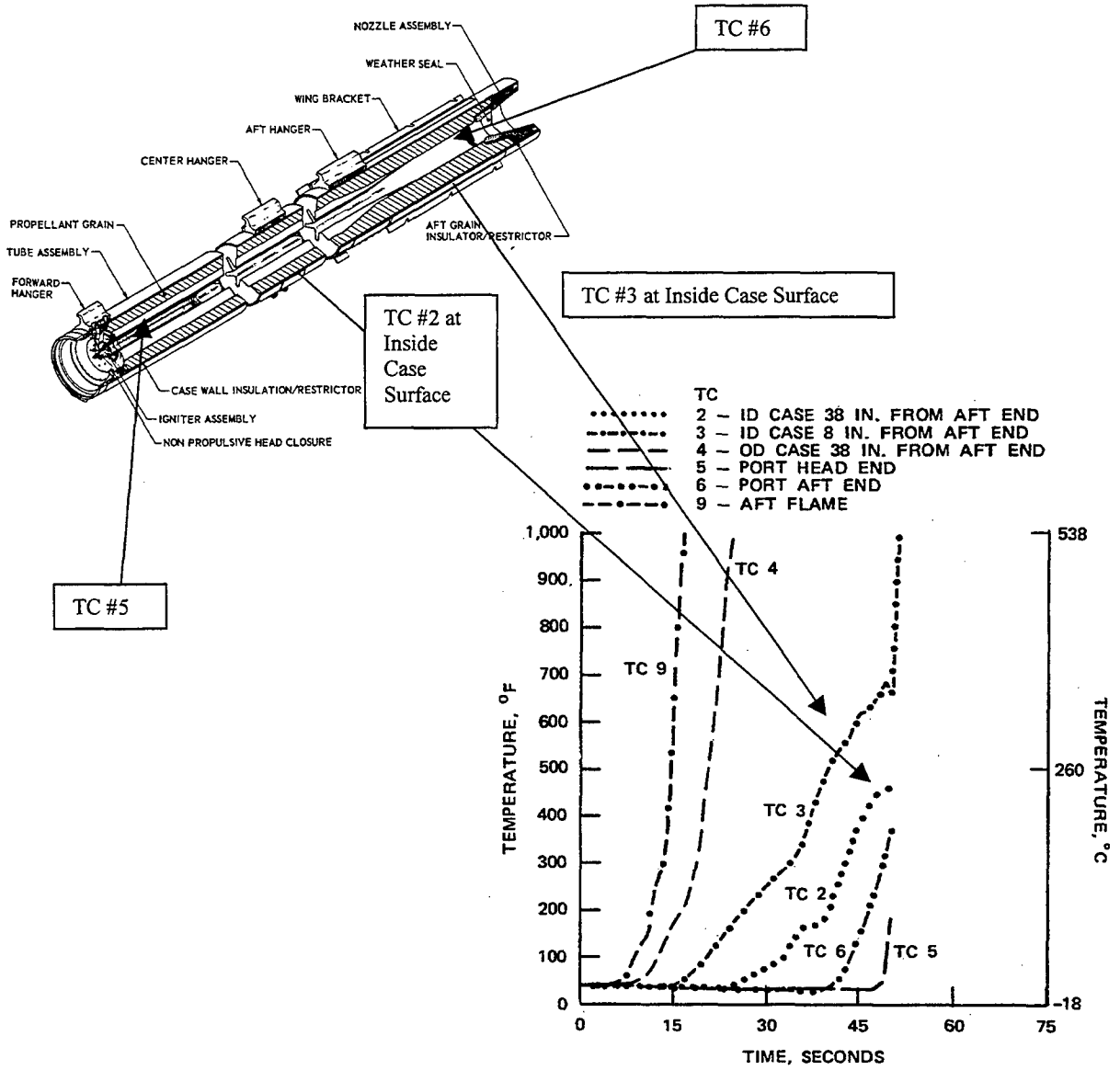

Figure 6. Temperature Spikes at Both Inside Case Wall and Propellant Grain Inner Bore Show Near Instantaneous Flame Spreading With Full Propellant Grain Ignition[1]

Farmer et al[5] and Rogerson[6] provided further evidence supporting the motor failure mechanism in full-scale rocket motor fast cookoff tests. Real time radiography was used to view case-liner debond evolution, bore collapse, and burn-back surfaces of the propellant grain, as well as simultaneous video (longitudinal through the nozzle) of center bore collapse behavior. Figure 7 shows a radiographic image of the formation of the case-liner debond during a test where the bore was simultaneously observed to collapse until the pressure was subsequently released through case failure. Other excellent diagnostic imagery can be found in videotape records of several tests[5] archived at CPIA.

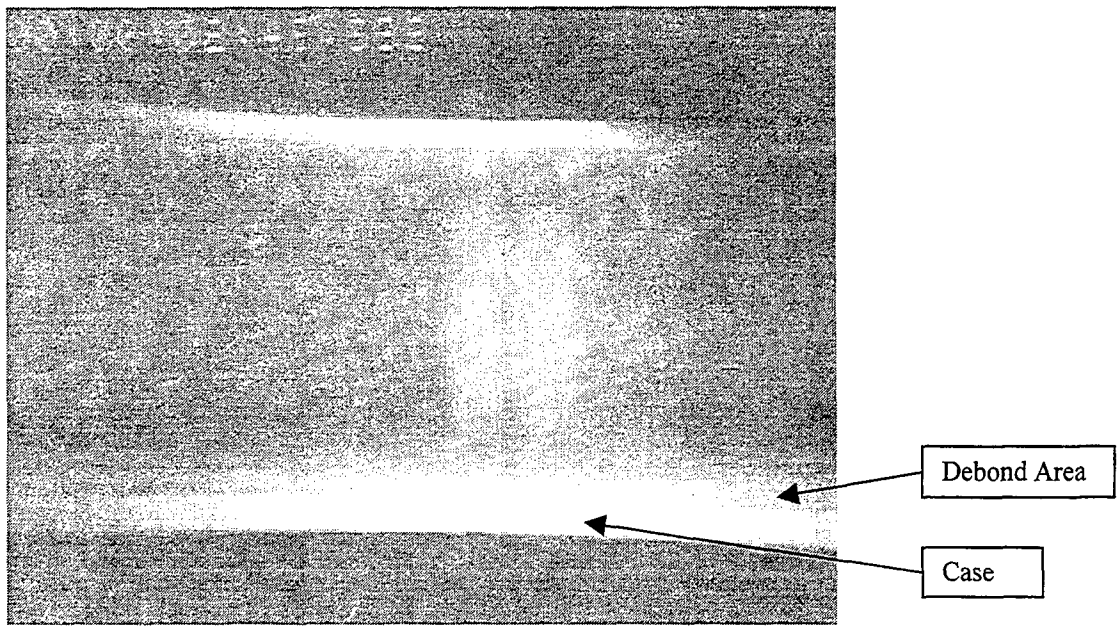

Figure 7. Radiograph (perpendicular to rocket motor axis) showing Case-liner Debond[6]. The debond is indicated by white shading between the motor case (very bright white) and propellant grain (dark). The vertical white shading in the center is an artifact.

Vetter[1] also reports the results of simultaneous case-liner-propellant bondline temperature measurements and pressure measurements at the case-liner bond and center bore areas during fast cookoff testing of analog motors. The analog motor assembly is shown in Fig. 8. Temperature and pressure transducer data for a test using a specially formulated liner and a typical reduced smoke propellant are shown in Figs. 9 and 10. The case-liner pressure increased sharply up to about 420 psig, then dropped somewhat. The bore pressure increased sharply as the case-liner pressure decreased, indicating that the bore was collapsing. Ignition on the grain outer diameter was observed from a sharp rise in temperature to propellant flame temperatures at the forward case-liner debond during bore collapse. Immediately following ignition, the case ruptured (as observed on videotape) releasing the pressure at both the case-liner bond and in the center bore. Burning (normal surface regression) proceeded from the outer grain diameter, through the propellant web, and finally into the inner bore at a much later time. In another test with fairly similar results, the investigators concluded that the lack of a temperature increase at the center bore during the transient ignition and case rupture process indicated that cracking of the grain did not occur (thus avoiding possible flame propagation into the center bore).

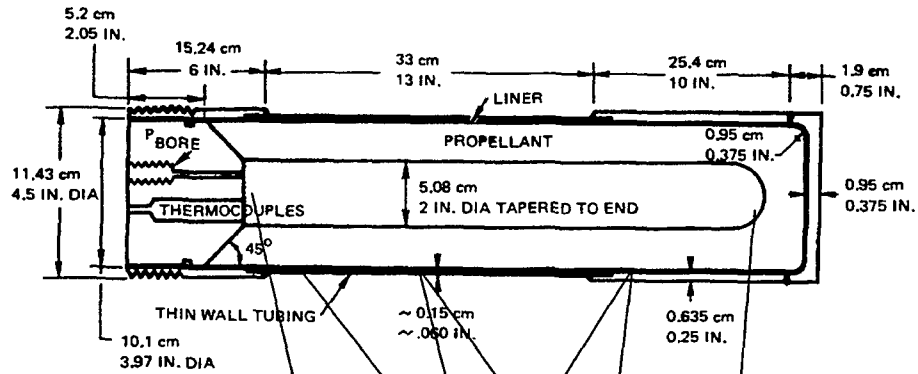

Figure 8. Analog Motor Assembly of Vetter[1]

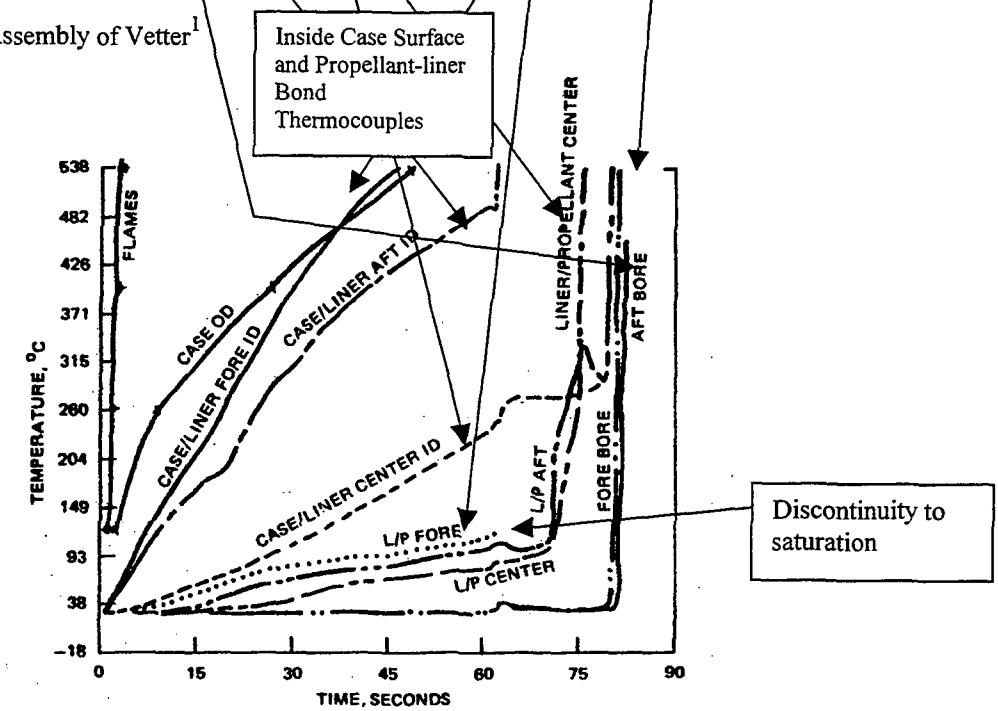

Figure 9. Case-liner Bond and Bore Temperature Traces Indicate Ignition on the Grain Outer Diameter[1]

Hicks[7] made strain gage measurements on an aluminum tube simulating the propellant inner bore of an instrumented analog motor (Fig. 11). In these tests, the inner aluminum "bore" was observed to buckle (partially collapse) due to the pressure generated at the case-liner debond area (Fig. 12). The strain gage measurements were used to estimate the pressure loading that caused buckling of the inner tube. Vetter[1,8] also reports the use of linear potentiometers on the inner bore propellant surface to identify bore collapse.

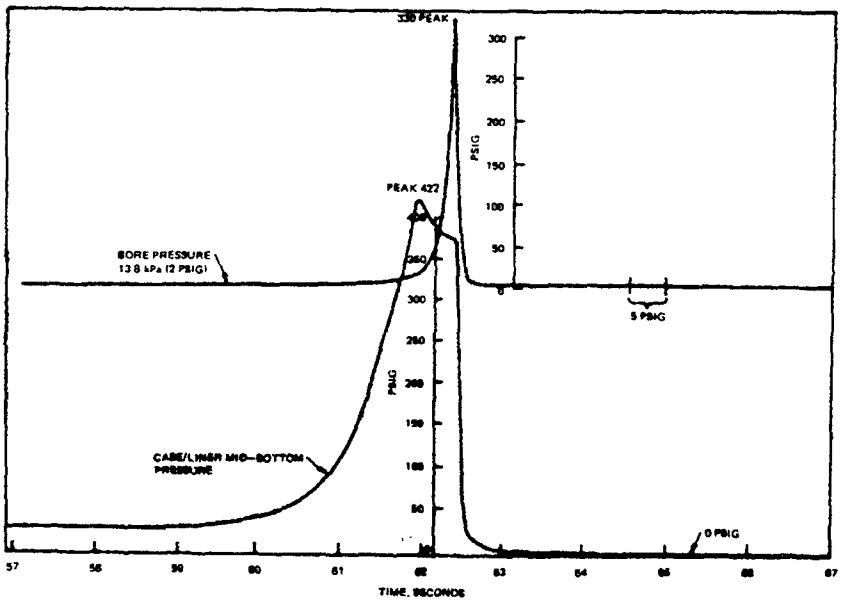

Figure 10. Case-liner Bond and Center Bore Pressure Traces Indicate Ignition on the Grain Outer Diameter[1]

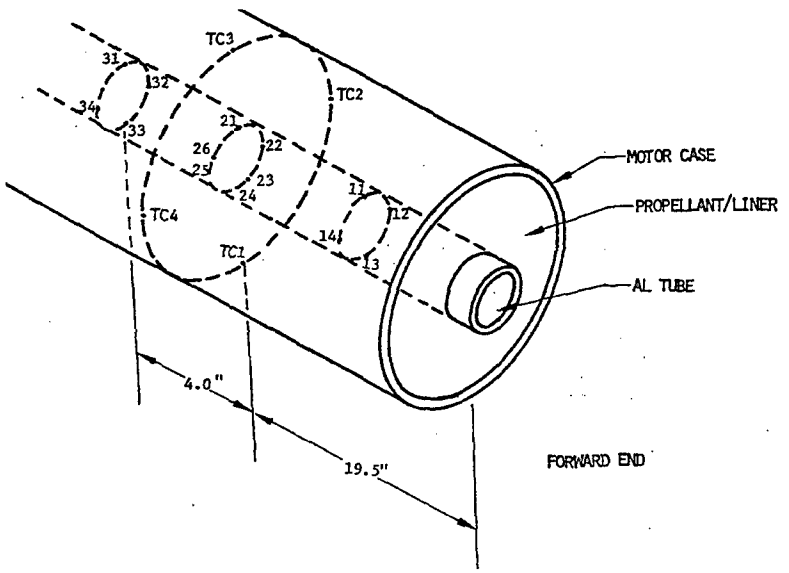

Figure 11. Instrumented Analog Motor[7]

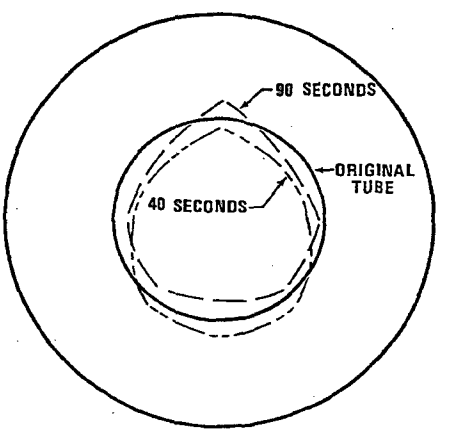

Figure 12. Cross Section of Inner Bore Deflections Due to Case Bond Pressure[7]

2.2 Laboratory Characterization of Liner Materials

Laboratory scale liner characterization tests may provide valuable information concerning case-liner bond failure behavior under fast cookoff. Vernon[9] and Vetter[1] used plate tests to examine liner thermal and physical behavior during cookoff. Liner samples were sandwiched between two metal plates and heated on one side using a propane torch. The rear plate often contained a hole in the center in order to observe liner bubble formation. A variety of liner physical behaviors, from complete liquifaction with formation of large bubbles - to formation of foamy tars, have been observed in these types of tests. Clark et al[2] used similar tests to investigate liner thermal and physical behavior during fast cookoff. Their test specimen was slightly more representative of an actual motor configuration, since it did not include a second (rear) plate (Fig. 13). Case-liner bubble formation was observed by stripping the secondary insulation layer in the latter part of the test. The author wonders if instrumented plate type tests (using a load cell or other strain/pressure gages at the rear insulation face) might provide additional, quantitative information for input into structural analyses.

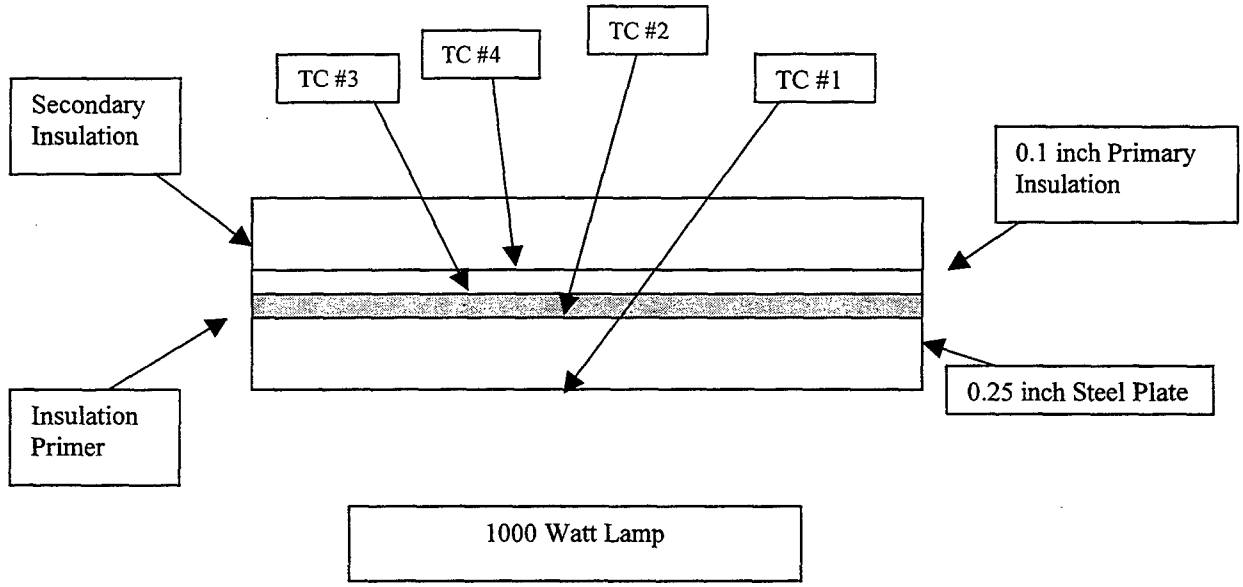

Figure 13. Plate Test Simulating Rocket Motor Bondline[2]

Standard thermal analysis techniques have also been used to understand liner behavior under cookoff conditions. Vernon[9] used DTA/TGA analysis and sealed vessel Parr bomb heating tests to examine thermal decomposition, mass loss, and pressure generation potential for various liner samples. Figure 14 shows that different liners have significantly varied pressure-generating capabilities during heating.

Clark et al[3] derived a thermal decomposition kinetic rate model for a specific liner using TGA measurements. The model was used to account for the insulative properties of the case-liner gas

gap formed in the early stage of fast cookoff. The TGA data were fitted to a first order Arrhenius rate expression

$$dx/dt = A\,(1-x)\exp(-E/RT)$$ where x = fractional conversion
E = activation energy (Btu/mole)
R = gas constant, 1.987 Btu/mole-R
A = Arrhenius pre-exponential factor (minutes^{-1}).

Sample curve fit data are shown in Fig. 15.

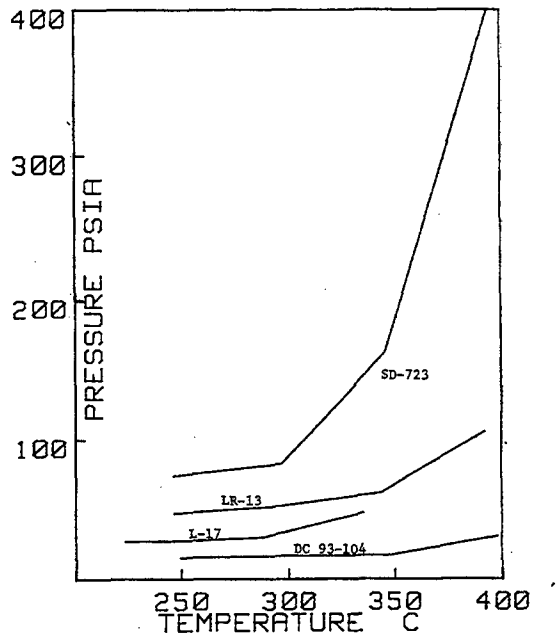

Figure 14. Pressure Generation for Various Liner Compositions From Confined Heating Tests [9]

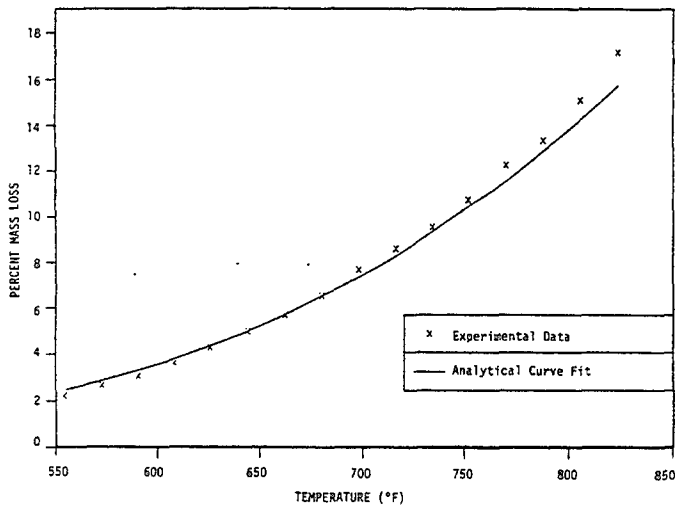

Figure 15. Decomposition (Mass Loss) Data for a Sample Propellant-liner [3]

2.3 Case-liner Physical Modeling

The liner characterization data can be useful as source input for case-liner pressure generation modeling, and subsequently through conventional SRM structural mechanics modeling, overall motor failure response in fast cookoff. Fong et al[10] developed a 1-D finite difference thermal model based on the SINDA code for predicting the pressure generated in the case-liner debond area from liner pyrolysis (or other phase changes) during motor fast cookoff. A series of equations for a finite number of thermal nodes containing moving boundaries are solved using physical and thermal properties of the liner and standard heat transfer analysis methods. The volume of pyrolysis gas generated in the case-liner debond area, the associated gas pressure in the debond, and finally, deflections of the case inner surface and propellant grain outer surface due to the gas pressure are calculated. The fundamental thermal node model setup is shown in Fig. 16.

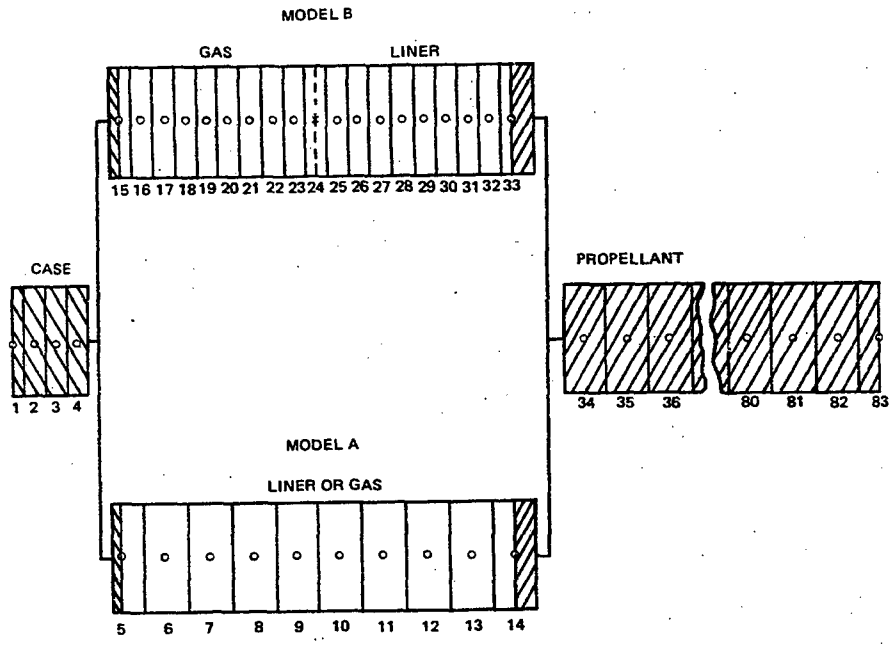

Figure 16. Thermal Node Model Structure for 1-D Rocket Motor Configuration [10]

The energy balance at each thermal node is calculated using the equation shown below:

$$m\, C_p\, dT/dt = k\, A\, \Delta T/\Delta X + Q$$

where
m = mass of the node
C_p = Specific heat
t = time
k = thermal conductivity
A = surface area
ΔX = heat path distance
Q = additional heat sources.

The left side of the equation represents the heat capacity of the node. The first term on the right side represents the thermal energy conducted in and out of the node. The second term on the right represents additional heat sources or sinks resulting from sublimation, internal decomposition, or other thermodynamic processes occurring with the liner contained in the node. Two alternate thermal nodal models describe the liner behavior. Model A consists of all liner or pyrolysis gas, representing the state of the liner prior to any phase changes or upon complete transformation to gaseous species. Model B consists of both gaseous and solid states, representing the intermediate stages of liner pyrolysis or phase transformation.

Liner decomposition and/or phase transformation are described by Arrhenius kinetics and conventional thermodynamics (heat generation/loss for these processes). Heat transfer processes (radiative and conductive) across the debond gas gap are also considered. Roark's equations for a cylinder are used with the ideal gas equation to compute the liner debond gas pressure and deflection of the outside liner surface away from the inside of the motor case[11].

Analog motor fast cookoff experiments were performed to test the model. The test concept, similar to that reported above by Hicks[7], consisted of an 8-inch diameter steel motor case lined with 0.05-inch layer of HTPB based liner and loaded with inert stimulant propellant (Fig. 17). Temperatures at the liner-propellant interface and propellant interior were monitored. Strain measurements induced on an aluminum tube simulating the propellant inner bore were also made.

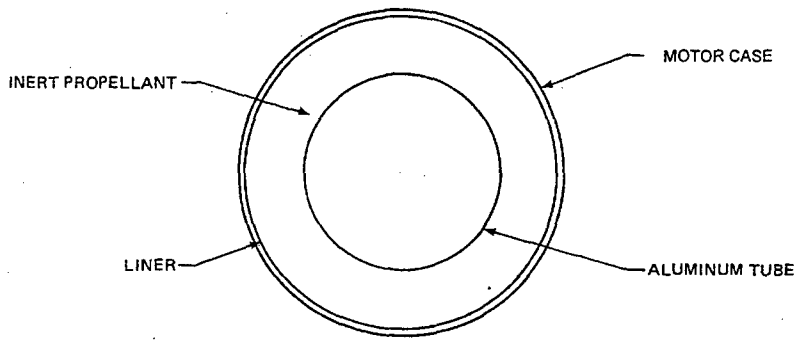

Figure 17. Test Motor Cross Section[10]

The liner pyrolysis gas was assumed to have the molecular weight and thermal properties of carbon dioxide. Arrhenius parameters and thermodynamic coefficients describing liner decomposition/phase transformation reactions were also specified (Table 1 and 2), but the author cannot verify if they were assumed or based on materials test data. Accurate input parameters could be obtained by using appropriate liner characterization test data (decomposition kinetics, gas generation, gaseous decomposition products, phase transformation thermodynamics by DSC, etc.) as discussed in preceding paragraphs.

Table 1. Heats of Vaporization Parameter for Two-liner Phase Transformations – Complete Liner Sublimation and/or Combined Liner Sublimation/Decomposition[10]

Temperature (°F)	Heat of Vaporization (Btu/lbm)	
	Complete Liner Sublimation	Sublimation plus Decomposition
400	+ 225	+ 100

Table 2. Arrhenius Parameters for Two-liner Decomposition Reactions[10]

Parameter	Reaction	
	A	B
Temperature (°F)	283	620
Initial Wt Fraction	0.1473	0.8527
Final Wt Fraction	0.0194	0.2771
Pre-exponential, 1/s	3.463 e^{-3}	5.383 e^{-3}
Activation Energy/Gas Const (E/R), (°R)	389	418
Reaction Order	1.667	1.709
Heat of Reaction (Btu/lbm)		
Decomposition Only	- 75	-150
Sublimation/Decomposition	- 25	- 100

Model predictions exhibited general trending agreement with the validation experiment. Figure 18 shows the predicted and measured liner-propellant interface temperatures. Figure 19 shows the experimentally determined case-liner debond gap pressure in the longitudinal middle/forward bottom area of the motor estimated from strain gage measurements at the inner bore. The maximum pressure rise rate was determined to be 5 psi/second. The pressure tail-off, after approximately 30 seconds, is due to development of a gas leak allowing the pyrolysis gases to vent from one end of the motor. Figure 20 shows the model prediction of case-liner debond gas pressure (the three different curves correspond to different assumptions associated with liner behavior – sublimation, decomposition, or a combination of the two). The predicted pressure rise rate was also about 5 psi/second, in good agreement with the experimental results, for boundary conditions where liner sublimation was used. (The time scales for the measured and predicted data are off set since the experimental data were initialized at the start of pressure rise. Accounting for this off set, the measured and predicted curves appear to overlap qualitatively).

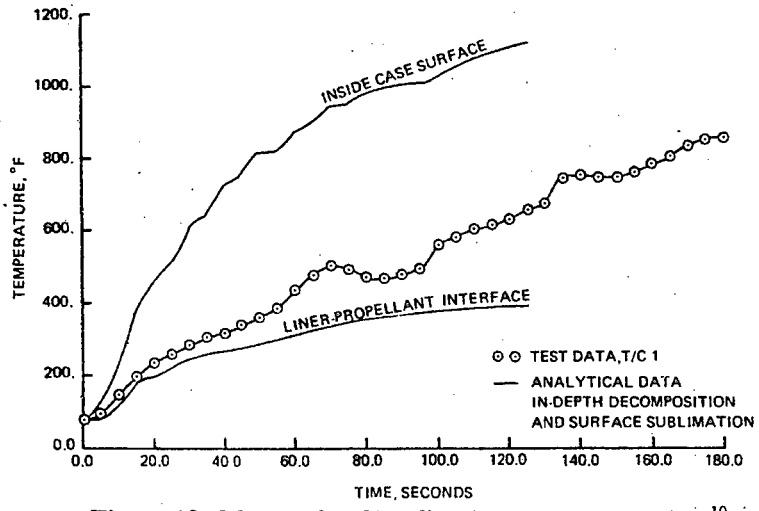

Figure 18. Measured and Predicted Temperature Profiles[10]

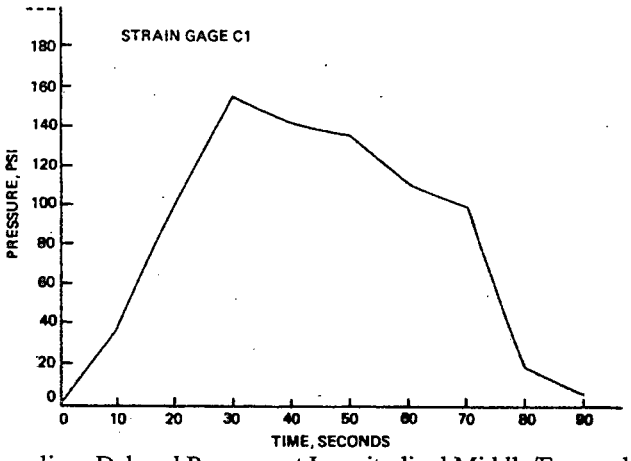

Figure 19. Measured Case-liner Debond Pressure at Longitudinal Middle/Forward Bottom Area[10]

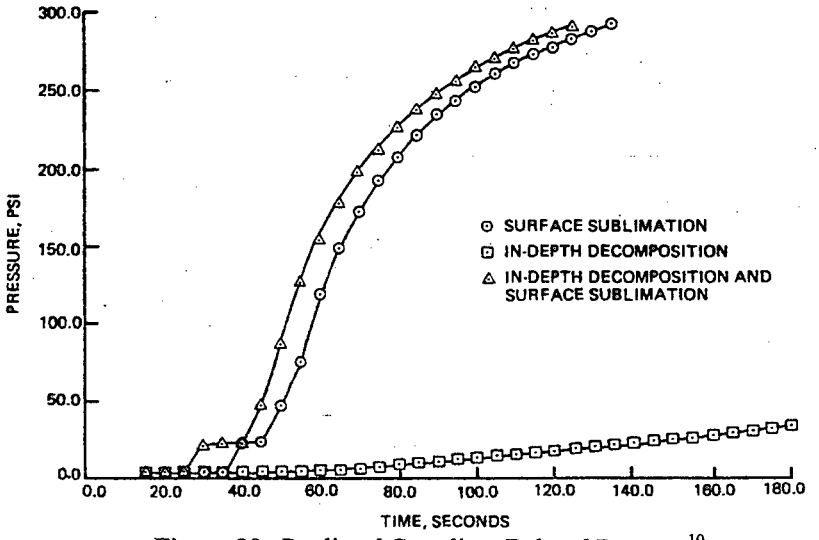

Figure 20. Predicted Case-liner Debond Pressure[10]

Additional model validation efforts, showing reasonable agreement, were reported with full-scale HARM rocket motor fast cookoff tests[8]. In the model predictions, experimental TGA and DSC data for the propellant-liner were used to obtain estimates of liner decomposition kinetics and thermodynamic phase transformation parameters.

Sensitivity analyses of various model parameters were also performed by Fung et al[10]. Parameters for the baseline case are shown in Table 3.

Table 3. Sample Baseline Model Parameters for Sensitivity Analysis[10]

Initial Temperature	75 °F
Outer Radius of Steel Motor Case	4.0 inch
Case Thickness	0.060 inch
Liner Thickness	0.030 inch
Propellant Web Thickness	1.91 inch
Inner Bore Radius	2.00 inch
Density of Case Material	0.280 lb/in^3
Density of Liner	0.0365 lb/in^3
Density of Propellant	0.0578 lb/in^3
Elastic Modulus of Case	3.0 e^7 psi
Elastic Modulus of Liner/Propellant	1.0 e^3 psi
Poisson Ration of Case	0.30
Poisson Ratio of Liner/Propellant	0.499
Molecular Weight of Liner Gas Products	45
Liner Heat of Reaction (Decomposition) Reaction A (endotherm) Reaction B (endotherm)	 + 25.0 Btu/lbm + 200.0 Btu/lbm

Figure 21 shows the sensitivity of model predictions for case-liner debond gas pressure as a function of the molecular weight of the liner pyrolysis gas (multiples of 0.5, 1.5, and 3 times the baseline molecular weight of 45g/mol). Figure 22 shows the effects of liner thickness (multiples of 0.5 and 2 times the baseline of 0.03 inches) on debond gas pressure. The model predicts that these two parameters could have a significant influence on debond gas pressure.

Some shortcomings in the model have been identified, including assumptions involving pyrolysis gas molecular weight, instantaneous liner separation from the case upon the beginning of liner pyrolysis, and one dimensionality. Simple predictions of propellant grain collapse (uniformly around the motor circumference) are based on axisymmetric assumptions; however, this is probably not realistic in many cases due to non-uniform heating effects (flame temperature variations) often observed in fires. On the other hand, simple geometric boundary conditions could be applied (to add quasi-two dimensionality) by weighting the model calculations towards specific sections of the case-liner system. Vetter[1] previously demonstrated the use of conventional structural analysis methods to calculate deformation of a rocket motor propellant grain due to pressurization of simple geometric sections of the case-liner bond (assumed to result from liner pyrolysis during fast cookoff).

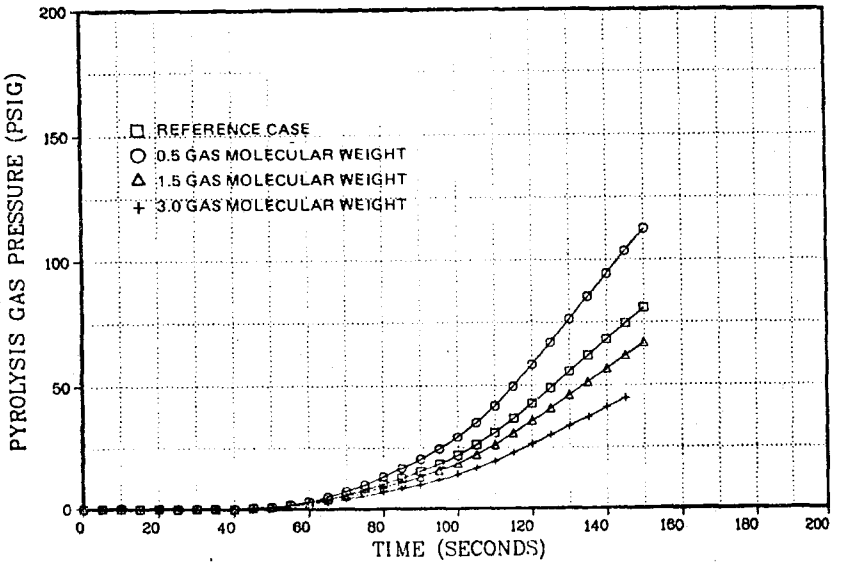

Figure 21. Calculated Liner Pyrolysis Gas Pressure as a Function of Gas Product Molecular Weight[10]

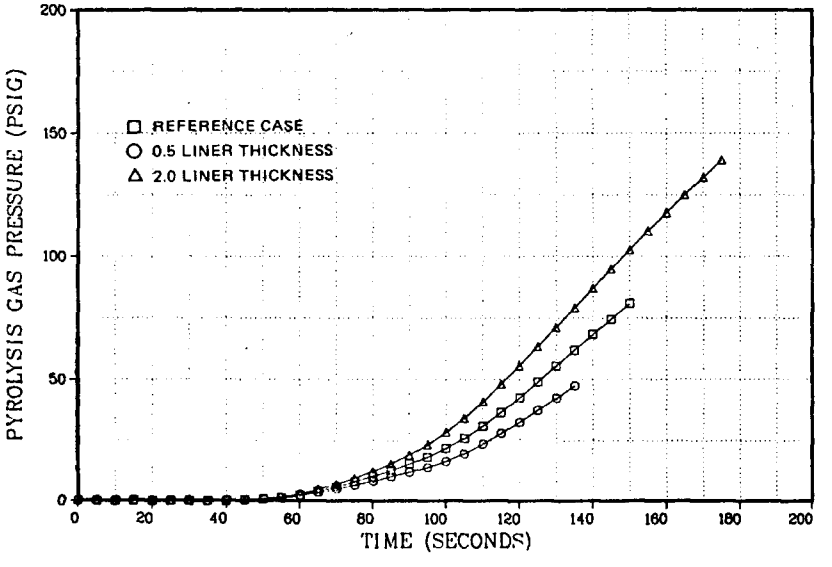

Figure 22. Calculated Liner Pyrolysis Gas Pressure as a Function of Liner Thickness[10]

Figure 23 shows a sample calculation of grain deformation due to pressurization of a 1/8-diameter section of case-liner debond. In this work, the pressurization profile was arbitrarily set to represent a typical fast cookoff test with an 8-inch diameter motor. Alternatively, a quasi-two dimensional pressure profile could be calculated using the model of Fung et al[10].

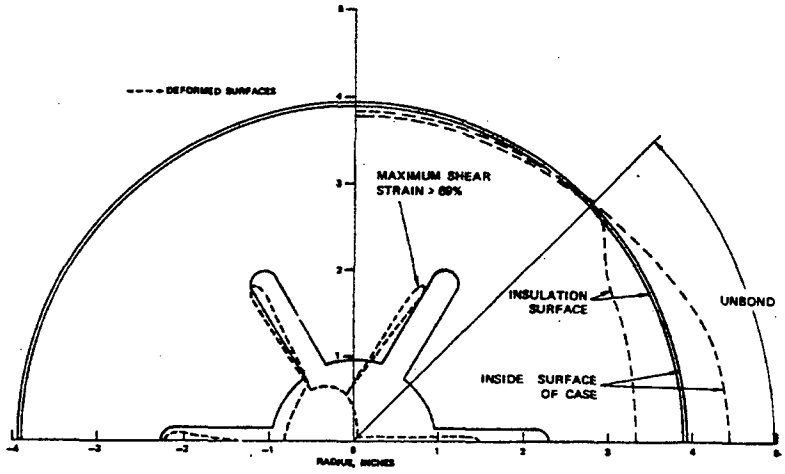

Figure 23. Calculated Deformation of Propellant Grain Half-Section Due to Pyrolysis Gas Pressurization at the Case-liner Interface[1].

Case-liner temperature and debond gas pressure distribution boundary conditions could also be derived experimentally. For example, in the validation experiments reported by Fung et al[10], inner bore strain gage data were used to estimate the liner debond pressure distribution around the motor circumference. Figure 24 shows the resulting (experimentally estimated) pressure distribution and calculated inner bore displacement around the motor circumference, at the longitudinal center of the motor. They hypothesized that the asymmetrical pressure distribution (Fig. 24) was directly proportional to an asymmetrical input temperature distribution around the external surface of the motor case supplied by the source fire. If this hypothesis is correct, one simple way to empirically determine appropriate boundary conditions involving case-liner debonding (areas or pressure distribution) for further structural modeling might be to obtain good temperature distribution data on the source fire and possibly external motor case surface in an inexpensive inert bonfire test.

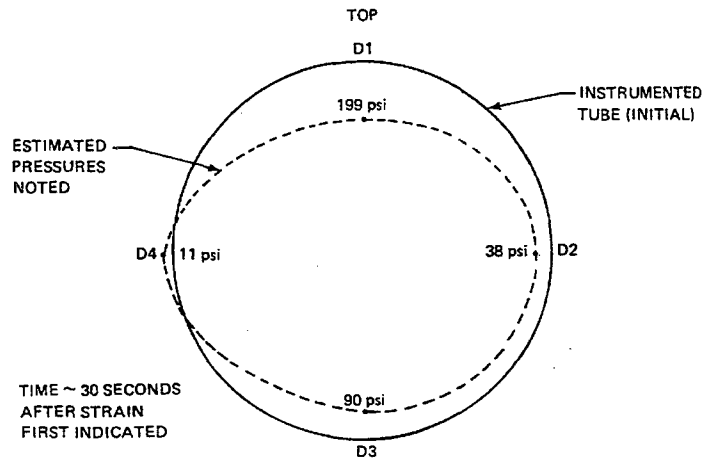

Figure 24. Experimentally Estimated Pressure Distribution and Inner Bore Displacement Around the Motor Circumference in Validation Tests of Fung et al[10] [Refer to Fig. 17 for Reference Motor Cross Section]

Victor[12] demonstrated a simplified one-dimensional numerical heat transfer analysis approach. Victor points out that 1-D analysis should be sufficient as long as there are no large flame temperature variations (criticality is not defined), or no other radial or longitudinal heat paths into the energetic material, and no important end heating effects. The model calculates thermal heat transfer through the case and liner to the outside diameter of the propellant grain, and uses Arrhenius decomposition kinetics for the propellant to predict ignition. Liner phase transformation/decomposition and gas generation effects are ignored in the model, per se, but can be estimated based on internal temperatures calculated from the heat transfer analysis.

The most sophisticated approach to better account for non-uniform heating effects associated with real cookoff scenarios might be to incorporate a fundamental heat transfer and/or case-liner physical model into a 2-D (or perhaps even 3-D) finite element or finite difference calculation framework in order to spatially define the case-liner temperature and debond gas pressure distribution, and the resulting stresses, strains, and case/propellant deformations. The Navy funded some additional research in the 1985 timeframe to investigate thermal and structural finite element modeling of motor fast cookoff using the NASTRAN code[13]. Although much was learned, problems in optimizing finite element arrays to capture both thermal and structural behavior were not overcome at that time. Thermal-chemical finite element modeling of rocket motors during fast cookoff (without consideration of structural response) was advanced using a modification of the Los Alamos National Laboratory 2DE code in an Army program conducted in the 1990 timeframe[14,15]. Liner pyrolysis effects were neglected and propellant ignition was calculated using simple global Arrhenius decomposition kinetics. Figure 25 shows the cross section and corresponding 2-D finite element model of an analog motor studied in the program. Results of validation testing showed good agreement with model predictions of temperature history at the internal motor case-propellant interface (Fig. 26).

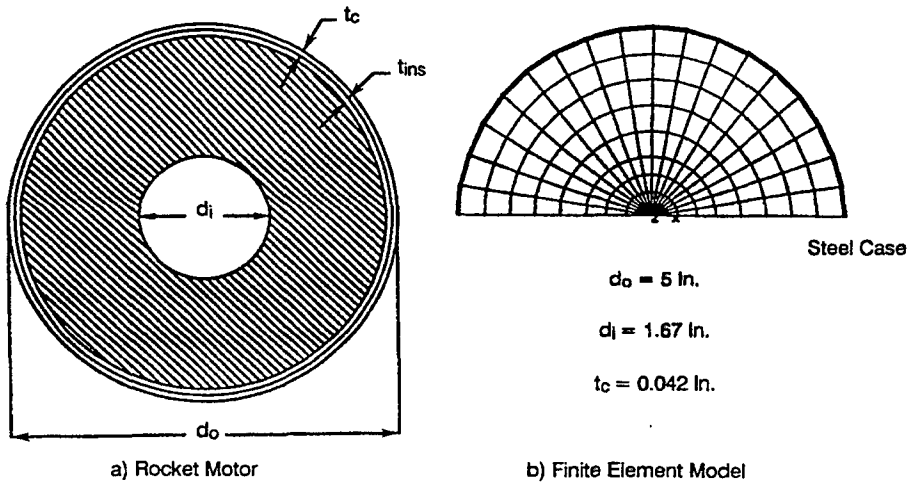

Figure 25. Cross-section and Corresponding 2-D Finite Element Calculation Mesh for Analog Motor Fast Cookoff Study[14,15]

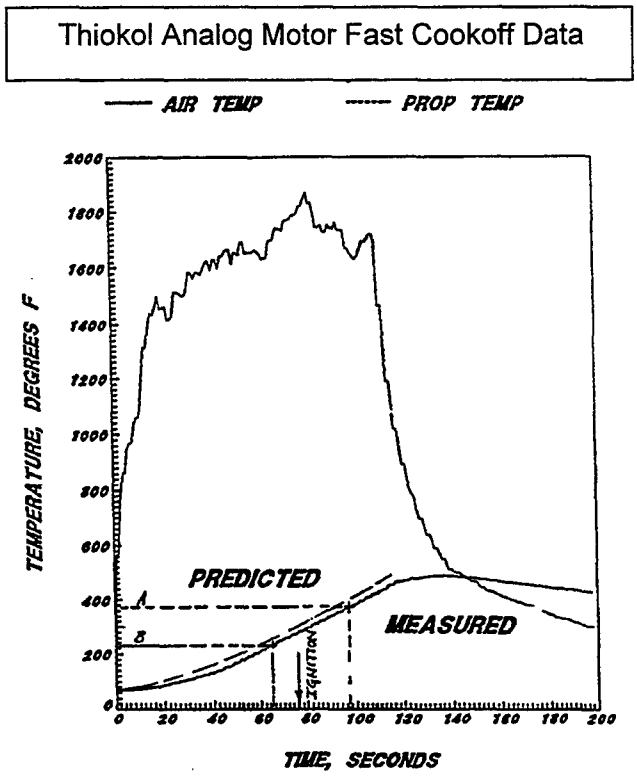

Figure 26. Predicted and Measured Thermal History at Case-propellant Interface[14,15]

3.0 PROPELLANT DAMAGE EFFECTS AND STRUCTURAL RESPONSE MODELING

Research data published by the propulsion hazards community has shown that creation of large burning surface areas, due to energetic material damage, will likely result in more violent response to unplanned ignition than undamaged material. Several investigators have considered structural damage of the solid propellant grain in their assessment of the hazard response of a rocket motor to accident stimuli. Leining et al[4] used this approach to assess the violence of a rocket motor reaction in an accident scenario involving crushing between an aircraft wing and aircraft carrier flight deck. Propellant strain-at-rupture data (from standard tensile testing) and predicted strain contours occurring in the motor were used to qualitatively estimate relative areas of damage in the propellant grain. Figure 27 shows a HONDO code finite element model of the scenario. Figure 28 illustrates predicted propellant damage cross sections for several different solid propellants. A primary observation from the model predictions is that extremely tough minimum smoke propellants (high allowable rupture strains) do not incur damage at the calculated strains, and thus were expected to show less violent deflagration reactions. Unfortunately, a full-scale experimental program was not conducted to verify the predictions.

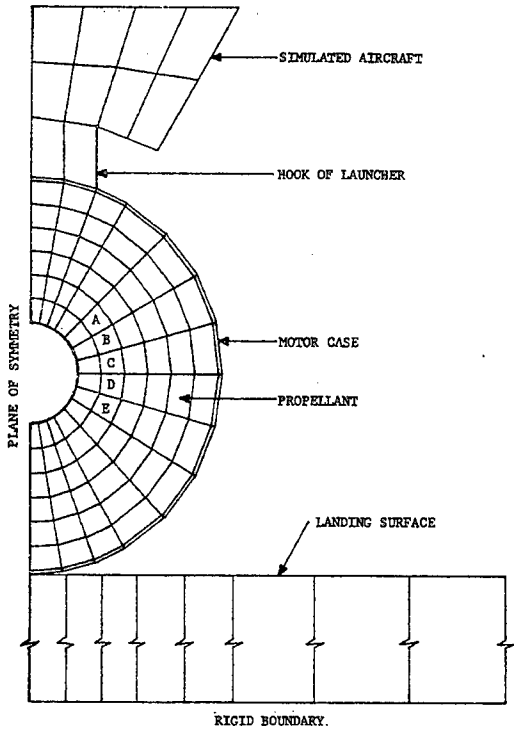

Figure 27. Finite Element Model of Rocket Motor Before Crushing[4]

———	Minimum Smoke (59 – 65 % total solids)
— . — . .	AP Reduced Smoke (87 % total solids)
.....	AP – HMX Aluminized (90 % total solids) (1)
- - - - -	AP – HMX Aluminized (90 % total solids) (2)

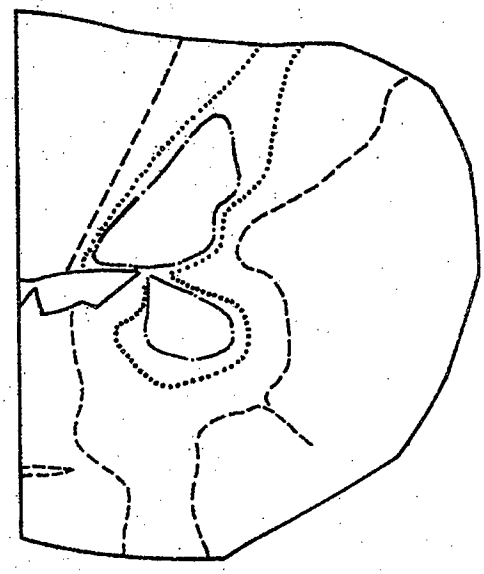

Figure 28. Propellant Damage Contours for Various Propellants[4]

Propellant damage/grain integrity effects were also evaluated in the assessment of deflagration-to-detonation transition (DDT) events associated with motor failures observed in early high-energy submarine launched ballistic missile (SLBM) developmental static test firings[16,17,18]. The damage model related the loads induced in several plausible motor malfunction mechanisms to the experimentally determined propellant mechanical properties in order to simulate the generation of damaged propellant areas. Propellant damage was also empirically evaluated using simulated (cold gas blow-down) failure tests with subscale analog motors and using shotgun/friability impact tests with propellant samples. Observations and data on propellant damage were explicitly coupled with ballistic (convective combustion) analysis on simulated damaged propellants to assess the DDT potential.

Two of the three most likely failure modes inferred from these events include some similarities to failure modes that may be important to the fast cookoff response of a rocket motor. The first credible failure mode involved generation of a damaged propellant bed at the case-propellant bond due to shear loads resulting from pressurized motor case failure, with subsequent DDT in the damaged bed[16]. While these motor detonations occurred with obsolete solid propellants having poor dynamic mechanical properties, one could imagine a similar failure mechanism during rocket motor fast cookoff, where bursting of the hot motor case occurs after flame propagates into the center bore. The failure mode is schematically illustrated in Fig. 29. Propellant damage in this scenario was characterized using cold gas blow-down tests with 10-inch and 30-inch diameter subscale motors by cutting the aft dome of the pressurized motor case with a linear shaped charge (Fig. 30; Fig. 31). Typical damage to the propellant grain is shown in Fig. 32. Damaged propellant from the case bond region was then burned in a closed bomb to examine burning surface area for assessment of DDT potential. Similar analog motor (hot) firing tests where the aft dome was cut with linear shaped charge during operation reproduced the detonation mechanism occurring in full-scale motors[19].

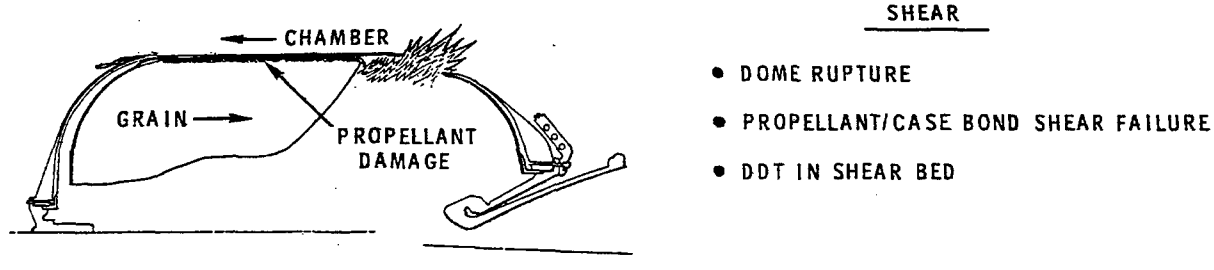

Figure 29. Large High Energy Motor Case Bond Shear Failure Mechanism Leading to Detonation[16]

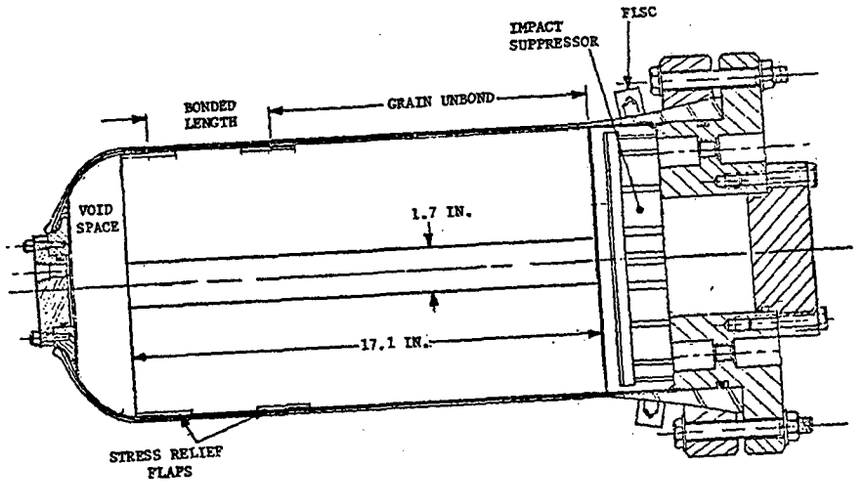

Figure 30. 10-inch Diameter Cold Gas Blowdown Analog Motor Test Apparatus[17]

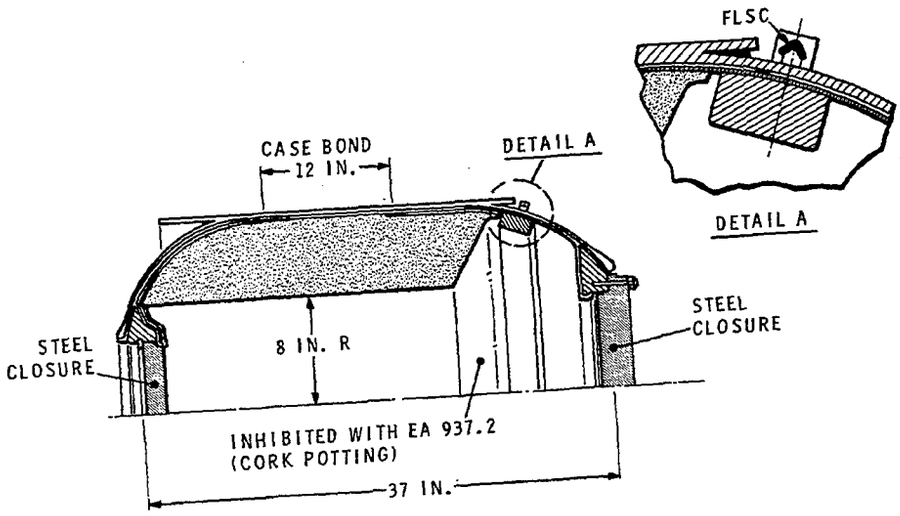

- CHAMBER PRESSURIZED TO 2000 PSI WITH HELIUM
- FLSC CUTS DOME 360°
- PREDICTED SHEAR STRESS = 750 PSI

Figure 31. 30-inch Diameter Cold Gas Blowdown Analog Motor Test Apparatus[16]

Figure 32. Cross Section Showing Propellant Grain Damage From 10-inch Analog Blowdown Test[17]

Since the initial DDT reaction in the damaged propellant bed propagated through the full, undamaged propellant mass in these motor failures, one can conclude that a damaged area of the propellant grain had dimensional area at some point greater than the critical diameter of the undamaged propellant (in order for the DDT reaction to serve as an explosive donor to the remaining propellant mass). The high-energy propellants used in these motors have relatively small critical diameters, typical of high explosives, on the order of less than 0.5 inches. Using this idea of structural damage characterization with respect to propellant critical diameter, one might be able to perform a qualitative assessment of detonation potential for rocket motor fast cookoff or other credible handling and storage accident scenarios as well. Obviously, as propellant critical diameter increases, the feasibility of detonation (through DDT) of a large motor decreases due to the necessity to damage larger and larger portions of propellant through credible failure modes.

Another potential failure mode of concern was implosion of the propellant grain due to pressures generated from flame propagation into the motor case-propellant bond area via propellant cracks or bondline flaws (Fig. 33), followed by DDT of damaged propellant in the center bore[16]. Propellant damage generated in this scenario was evaluated from structural analysis calculations and from an analog implosion test. The test vehicle (Fig. 34) is pressurized on both inside and outside grain surfaces, then the pressure is released from the center bore area by breaking a rupture disk. An example of propellant damage induced in one implosion test is

shown in Fig. 35. Again, this type of failure test could be representative of some failure modes occurring under fast cookoff conditions.

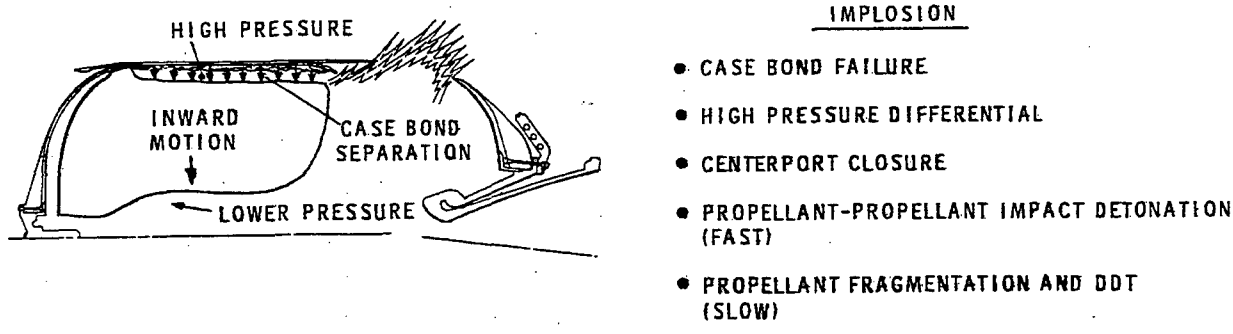

Figure 33. Possible Grain Implosion Failure Mechanism Leading to Detonation[16]

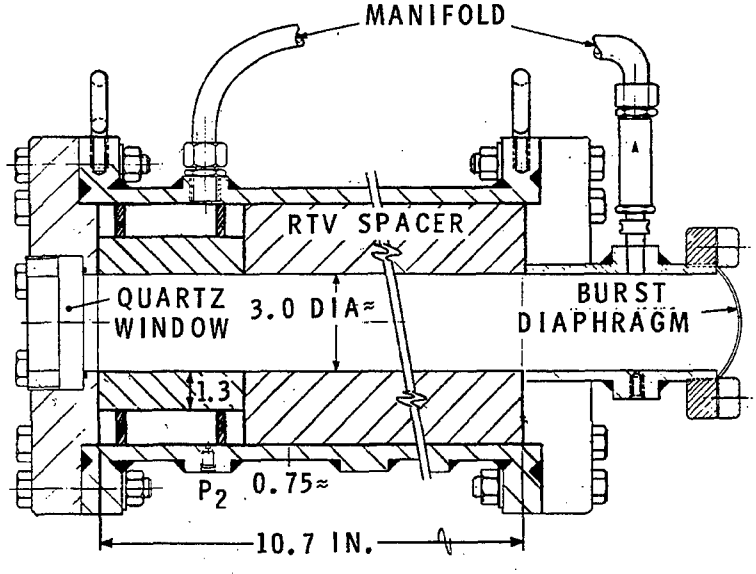

Figure 34. Analog Propellant Grain Implosion Damage Assessment Test[16]

Figure 35. Cross Section Showing Propellant Grain Damage From Implosion Test[16]

Structural response modeling and analog and full-scale replicate testing were also used to characterize the failure response of a large Pershing II first stage rocket motor due to accidental electrostatic discharge[20,21]. The structural response of the motor appears to be quite similar to the typical motor fast cookoff failure sequence. The failure sequence is illustrated in Fig. 36. In this accident, an electrical discharge occurred in the motor case – propellant bond region in the aft end of the motor. The discharge resulted in propellant ignition and flame propagation on the outer grain diameter, with subsequent gas pressurization between the propellant grain and motor case. The stress from pressurization in the case bond region caused unzipping of the case – propellant bond, and significant grain deformation/collapse resulting in closure of the internal motor bore. Ultimately the motor ruptured violently in the aft dome area due to propellant deflagration (as opposed to detonation), expelling the aft dome/nozzle assembly (the composite motor case was not likely weakened to an extent that might be expected in a bonfire scenario). Structural modeling was successfully used to determine the most probable origin (ignition point on the grain exterior) and evolution of the high pressure debond gas pocket, to characterize grain deformation, and ultimately to relate the structural failure with resulting debris observed in the accident[21]. Unfortunately, details of the modeling analysis have not been identified in CPIA literature.

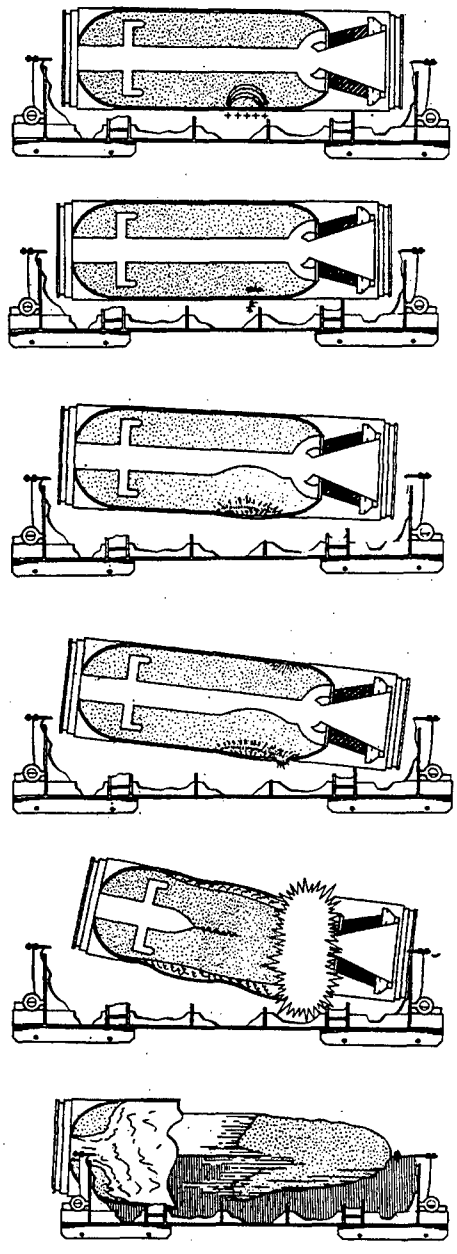

Figure 36. Failure Sequence in Pershing Rocket Motor ESD Incident[22]

Propellant grain implosion and case – propellant bond unzipping due to burning on the grain exterior were also investigated with subscale analog and full-scale Pershing motor tests. In these tests, which used dissected motor segments, cylindrical subscale models, and full-scale motors, the outer grain exterior was ignited using a hotwire or squib and small pyrotechnic charge implanted in the case bond area. Diagnostics used in the full-scale motor tests included fiber optic and radiofrequency sound sensor arrays (originating from the point of ignition) placed in the case bond region and on the motor case, respectively, to detect the growth of the case – propellant debond, as well as a pressure transducer placed in the motor center bore (increase in bore pressure indicated bore collapse).

The Pershing incident illustrates the opposite extreme (compared to the SLBM motor detonations discussed previously) with respect to the effect of critical diameter on motor hazard response. Conventional ammonium perchlorate based propellants such as the one used in the Pershing motor have very large critical diameters, on the order of several feet. Thus, even if a DDT reaction could have been initiated in a damaged propellant bed area of the propellant grain (which is extremely unlikely - requiring a substantial reduction in critical diameter for damaged propellant), the damaged area would have to cover an extremely large area in order to serve as a donor for detonation propagation into the pristine propellant.

4.0 COUPLED THERMAL-CHEMICAL-MECHANICAL COOKOFF MODELING

A complete finite element or finite difference model for describing rocket motor fast cookoff involves coupling of models characterizing 1) heat transfer and thermal/physical response of case and liner; 2) propellant thermal decomposition and pre-ignition chemical reactions; 3) structural mechanics of propellant grain and motor case deformation, propellant damage generation, and case-liner bondline peeling; and 4) ballistic or hydrodynamic response of the sustained propellant reaction. A coupled model translates the results of cookoff phenomena (heat transfer/thermal decomposition/ignition/initial burning) into hydrodynamic calculations, allowing prediction of the mechanical response of case confinement (case expansion velocity, fragmentation, etc) in a manner similar to the solution of standard detonation problems. Knowledge of the structural failure (propellant-liner debonding, propellant cracking, etc.) is required in the hydrocode analysis to predict flame propagation upon ignition and thus characterize case pressurization and ultimately the violence of the reaction. Since it is generally accepted that heat transfer and thermal-chemical analysis methods are relatively mature, this section emphasizes advances particularly involving structural and hydrodynamic aspects of the cookoff problem.

4.1 Hydrodynamic Modeling of Explosive Systems

Hydrocode modeling of reactive flow using a pressure-based initiation/burn equation (governing the transformation of un-reacted energetic material to its decomposition products and associated energy release) is a well-established analysis capability for examination of detonation phenomena[23]. For example, motion of the walls of a copper tube in the standard cylinder expansion test (for evaluation of explosives performance) can be accurately modeled with a hydrocode calculation. Figure 37 schematically illustrates the wall expansion observed in a typical cylinder test. Figure 38 shows DYNA2D modeling output for the test[24]. As another example, Fig. 39 shows the (quantitative) predicted and experimentally determined wall velocities for cylinder expansion tests with an aluminized plastic bonded explosive containing ammonium perchlorate[25].

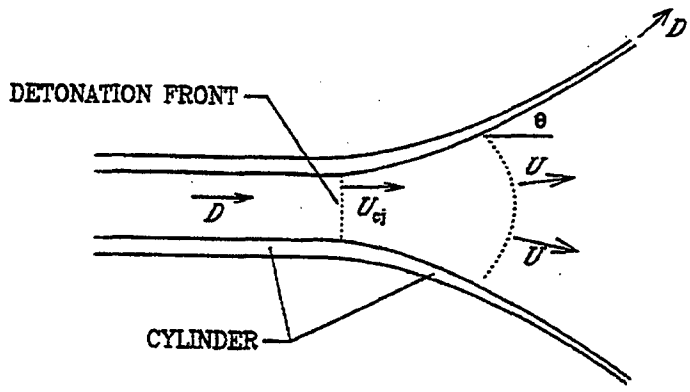

Figure 37. Schematic of Cylinder Expansion Test in Reference Frame Moving at Detonation Velocity D[24]

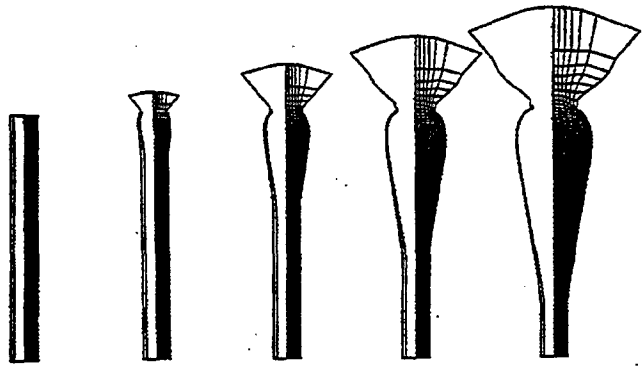

Figure 38. Hydrocode Modeling of Typical Cylinder Expansion Results at 6 microsecond Intervals[24]

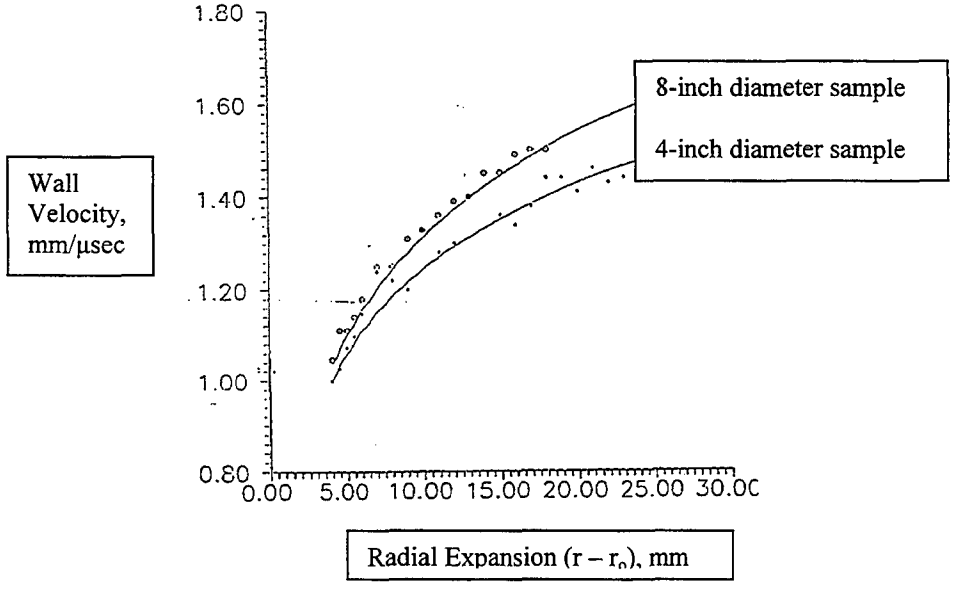

Figure 39. Cylinder Expansion Wall Motion Results [Experimental (points) and Calculated (lines)] for Aluminized Explosive Containing AP[25]

Reduced energy release (sub-detonation) behavior characterizing the transformation of un-reacted energetic material into reaction products can also be built into a hydrocode model. For example, in a major (multi-million dollar) program, Lawrence Livermore National Lab developed the Propellant Energetic Response to Mechanical Stimuli (PERMS) model, implemented in the CALE finite difference hydrocode, to model the sub-detonative propellant explosive burn reaction resulting from impact[26,27]. The model includes algorithms to characterize both reactive shock/decomposition/combustion and mechanical response (shock induced propellant fracture, etc) aspects of the propellant reaction. Energy release in the hydrodynamic analysis is calculated using a modification of the Lee-Tarver ignition and growth framework, where initiation is expressed in terms of shock wave compression and growth of reaction is expressed as a two-stage pressure based propellant combustion reaction applied to small, initially isolated grains burning inward from the surface. The two stages of combustion include: a) oxidizer (in this case ammonium perchlorate) decomposition and subsequent reaction with binder components modeled using a conventional $r = bP^n$ burn rate law; and b) reaction of the aluminum fuel component with the oxidizer-binder intermediate products to form final reaction products, modeled using an independent pressure dependent rate law. A propellant fracture model that computes enhanced surface-to-volume ratio of the burning propellant, based on applied impact-induced strain and strain rate, is also incorporated. These concepts are implemented as equations describing the rate of change in extent of reaction of the form

a) for the oxidizer-binder reaction to intermediate products,

$$d\lambda_1/dt = I\,(1-\lambda_1)^a\,(\mu-c)^b + G_1\,(1-\lambda_1)^d\,\lambda_1^e\,B\,P^n + A\,(e-e_o)\,\{\dot{e}\}\,(1-\lambda_1)^d\,B\,P^n$$

where the first term addresses initiation due to shock compression (μ);
$(1-\lambda_1)^d\,\lambda_1^e$ represents growth of reaction due to isolated grain burning;
$B\,P^n$ is a conventional propellant burning rate functionality;
$A\,(e-e_o)\,\{\dot{e}\}$ represents increased burning surface/volume ratio due to impact-induced damage created as a function of maximum applied strain above a damage threshold ($e-e_o$) and strain rate $\{\dot{e}\}$.

b) for the aluminum reaction with intermediates to form final products,

$$d\lambda_2/dt = G_2\,(R\lambda_1 - \lambda_2)^f\,(1-\lambda_2)^d\,p^{0.3}.$$

Model parameters for these equations were fit from a variety of small-scale tests and standard computational methods.

The PERMS model calculates the macroscopic propellant energy release as a function of time, ultimately for use in computing explosion parameters (blast wave characteristics and metal case acceleration). The PERMS model accurately reproduced explosive blast characteristics observed in large-scale explosive donor and impact tests with a typical ammonium perchlorate based composite propellant. The model also qualitatively captured the expansion behavior of an aluminum shell surrounding a 60-inch diameter propellant cylinder (analogous to the small-scale cylinder expansion test) when the sample was initiated in an explosive donor test (Fig. 40).

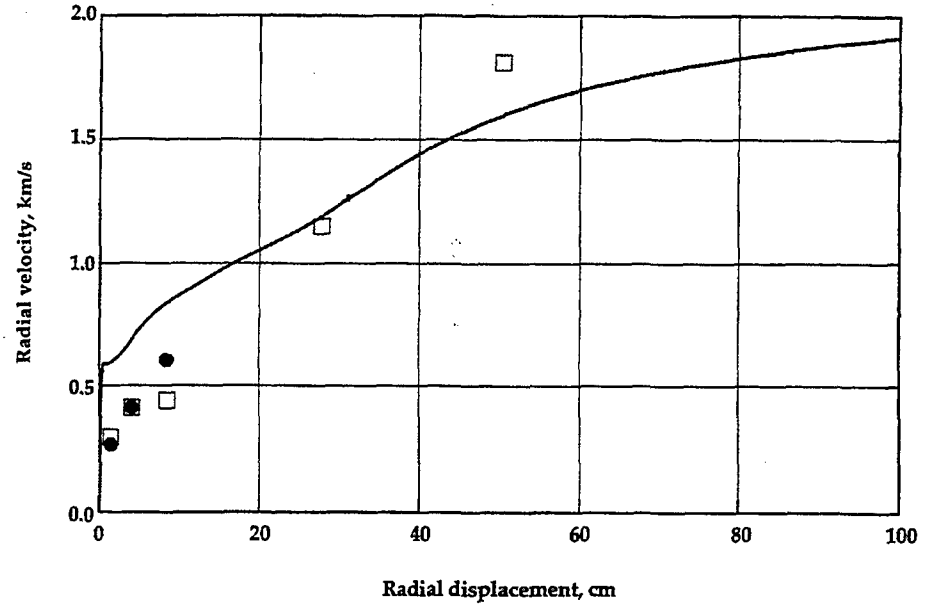

Figure 40. Radial Expansion of Aluminum Band [Experimental (points) and Calculated (lines)] Surrounding 60-inch Critical Diameter Test Sample[27]

Computational methods using sub-detonation energy release are also being developed and applied directly in hydrocode analysis of cookoff scenarios.

4.2 Cookoff Modeling

Raun et al[28] outlined a coupled finite element approach in the construction of a complete cookoff model using existing codes such as TOPAZ to characterize heat transfer and pre-ignition chemical reactions, coupled with the DYNA2D hydrocode to characterize transient combustion and structural dynamics of the motor case and propellant grain. A schematic representation of the modeling sequence is shown in Fig. 41. The heat transfer model uses simple global Arrhenius decomposition kinetics for the propellant. Reaction rates and energy release are determined in the hydrodynamic calculations using a simple propellant combustion burn rate law ($r = bP^n$) only. When the internal pressure (determined in the hydrodynamic calculation) is predicted to exceed the case burst strength, the calculated pressure and pressurization rates are input to an empirical fragmentation model to estimate reaction violence, which is defined by case fragment size and energy/velocity using empirical data from pressure vessel fragmentation characteristics. Unfortunately, full development and validation of the proposed model concept was not pursued.

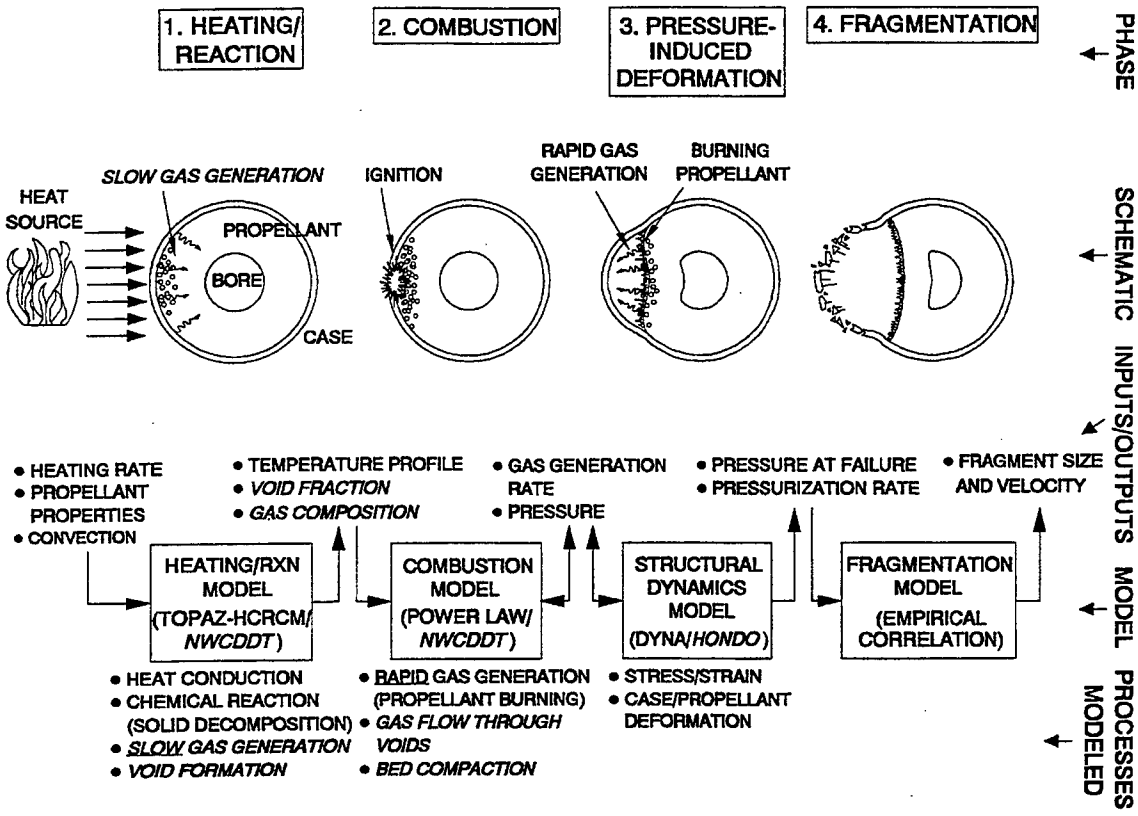

Figure 41. Cookoff Modeling Approach of Raun et al[28]

Victor[12] developed simple physical descriptions of bulk pressure generation and propellant combustion gas venting to estimate reaction violence for slow cookoff situations, which are probably applicable to many fast cookoff/bonfire scenarios as well. Victor cautions that a violent case burst response can be obtained from rapid pressurization, even under conditions where the case has become vented (or for that matter, under normally vented conditions associated with the presence of a rocket motor nozzle), due to flow chocking which might occur from nozzle blockage (from propellant expansion and/or deformation), or due to rapid gas generation from combustion of damaged propellant with increased burn surface area. The fundamental equation for the rate of pressure build up is –

$$dP/dt = ((dm/dt)_b - (dm/dt)_v)\, RT/MV$$

where M = average molecular weight of product gas

V = gas volume within case, which increases with time as $dV/dt = dm/dt_{(produced)}/\rho_p$

ρ_p = propellant density

$(dm/dt)_b$ = mass production rate from burning surfaces ~ $K\, A_{bo}\, a\, A_b(P,t)\, \rho_p\, P^n$

where $A_b(P,t)$ is a multiplier to account for increasing burn surface area with time, with A_{bo} equal to initial burning surface area at time of ignition

$(dm/dt)_v$ = mass flow rate from vents = $A_{vent}\, P\, k \sqrt{\{[2/(k+1)]^{(k+1)/(k-1)}\}}/\sqrt{(kRT)}$

where k = ratio of specific heats of product gas.

These equations might be useful in a simplified fragmentation analysis similar to the concept proposed by Raun et al[28].

Coupling of multi-dimensional thermal-chemical, mechanical, and ballistic/ hydrodynamic finite element/finite difference modeling codes has advanced significantly over the last few years, due in part to substantial research investments in the development of slow cookoff modeling capabilities[29,30]. In many respects, coupled modeling of fast heating scenarios should be more tractable, since significant heating of the bulk interior energetic material does not occur prior to ignition. A major hindrance to the advancement of slow cookoff models has been development of constitutive physical models of damaged energetic materials subjected to high temperatures for extended times[31,32]

Compton[33] successfully demonstrated some elements of a coupled thermal-mechanical-hydrodynamic modeling approach to predict the fast cookoff response of an explosive warhead. A commercially available computer aided engineering (CAE) finite element code was used to generate the thermal profile, extent of thermal decomposition, and thermal stress distribution prior to ignition. The results of the thermal analysis were used as input for a hydrodynamic analysis using the SPHT2D hydrocode. The hydrodynamic analysis used a conventional Arrhenius thermal explosion burn law, as opposed to a detonative pressure based initiation equation[34,35], to essentially distinguish between a laminar type burning reaction and a thermal explosion. According to Mader[34], the Arrhenius burn law expresses the extent of reaction (or conversely, mass fraction of un-reacted energetic material, W) between time steps n and n+1 as

$$W^{n+1} = W^n - \Delta t\, Z\, W^n\, e^{-E/RT}.$$

Model calculations were compared to analog warhead fast cookoff tests using three different explosives – two typically considered as insensitive munitions plastic bonded explosive (PBX) fills, and one melt cast explosive fill that generally yields violent cookoff responses. Calculations easily distinguished the burning type responses observed with the two IM filled warheads (where the model output was indicative of slow reaction growth at all points in the energetic material), compared to an explosion type response with the non-IM fill (where the model output was indicative of a thermal explosion). Figure 42 shows the pressure distribution derived from the thermal stress state calculated for the non-IM filled warhead at the time of thermal runaway. Figure 43 shows the pressure distribution calculated at about two microseconds into the hydrodynamic analysis. The hydrodynamic analysis indicates the creation of very high pressures representing the initiation of a violent thermal explosion originating at the bottom-most outer radius of the explosive charge. Similar plots for one of the IM filled warheads show significantly lower pressures due to the (pre-ignition) thermal stress state and also during the early phase of reaction growth in the hydrodynamic analysis.

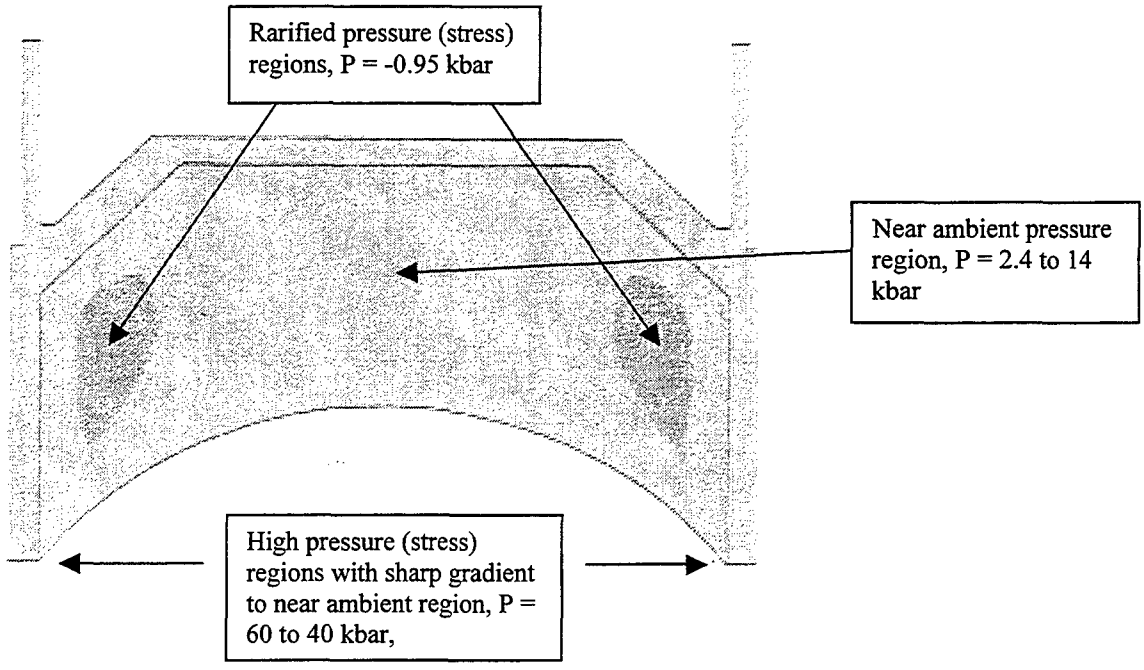

Figure 42. Calculated Thermal Stress (Pressure) Distribution in Melt Cast Explosive Filled Warhead Immediately Before Ignition[33]

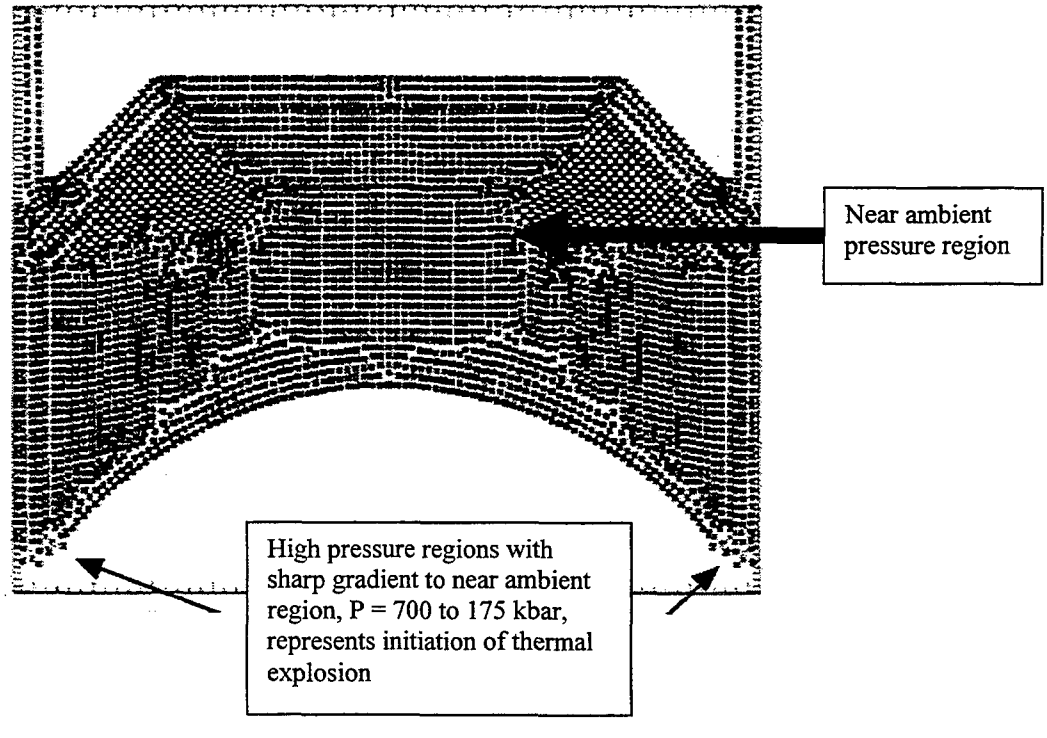

Figure 43. Calculated Pressure Distribution in Melt Cast Explosive Filled Warhead at 2 microseconds after Ignition[33]

Three state-of-the-art approaches to coupled thermal-mechanical-ballistic/sub-detonation hydrodynamic modeling of the entire cookoff process have been demonstrated in slow cookoff programs. These more sophisticated models attempt to capture all physical aspects of the cookoff process, including heat transfer, thermal properties of the energetic material at abnormal temperatures and pressures, chemical decomposition and thermal damage (prior to ignition), static and dynamic mechanical properties of the damaged energetic material, and hydrodynamics of the reaction propagation.

Sandia National Laboratories has coupled existing computer programs for thermal-chemical analysis (COYOTE), quasi-static mechanics (JAS3D), dynamic mechanics (ALEGRA), and shock physics (CTH)[30,36,37] . Reaction rates and energy release in the ALEGRA hydrodynamic analysis are calculated using a pressure dependent combustion law of the fundamental form ($r = bP^n$), which includes an additional parameter addressing the effects of thermal damage (increased burning surface area from porosity) developed in the energetic material due to chemical decomposition prior to ignition[32,38]. The burn model equation is of the form

$$r = (T/T_o)^\sigma (1 + \beta\lambda)\, b\, P^n$$

where $(T/T_o)^\sigma$ covers temperature effects on burning rate;
$(1 + \beta\lambda)$ represents increased burning surface area due to damage induced through thermal decomposition, where λ is a measure of the extent of decomposition prior to ignition.

Lawrence Livermore National Laboratory has modified a single hydrodynamic code (ALE3D) to accomplish all of the same calculations[30,39,40]. The third approach uses a combination of MSC/Thermal and NIKE2D codes to calculate initial thermal and mechanical conditions, coupled with the SPHT2D hydrodynamic code to investigate reaction propagation[29]. Detailed descriptions of constitutive mechanical relationships and hydrodynamic burn models used in these schemes have not been published in the CPIA literature.

These models are being evaluated for predictive fidelity in small-scale slow cookoff tests using a number of pipe bomb test fixtures. Figure 44 illustrates one generation of pipe bomb apparatus. Figure 45 shows experimental and modeling results from Sandia National Laboratory characterizing vessel expansion/deformation observed at early (pre-fragmentation) times in this test[30]. The coupled thermal-mechanical/hydrodynamic model qualitatively agrees with the deformation features of the confining pipe walls observed using flash X-ray techniques in the experiment. Deformation of the copper end plugs is predicted; however, such behavior is not observed in the experiment.

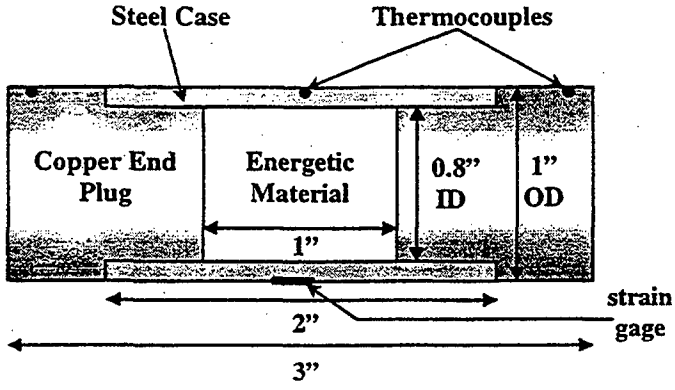

Figure 44. Small-scale Slow Cookoff Pipe Specimen[30]

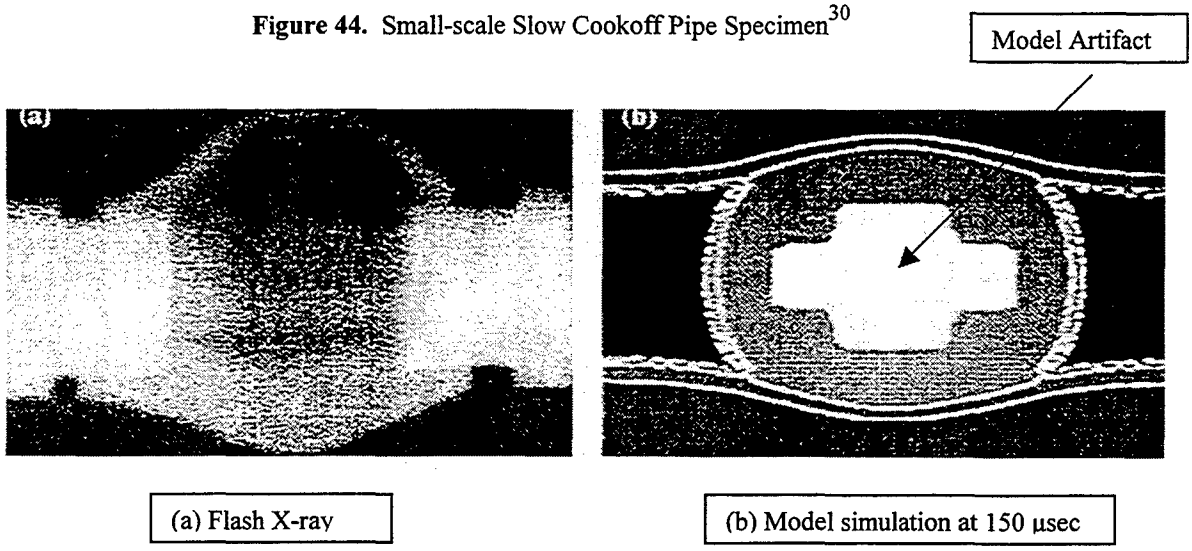

Figure 45. Experimental and Calculated Deformation of Slow Cookoff Pipe Specimen[30]

More recent experimental and modeling results for a slightly modified pipe bomb test (Fig. 46) have also exhibited qualitative agreement (Fig. 47a and Fig. 47b). In this test, deformation and subsequent rupture occurred in the middle section of the pipe with little deformation towards the ends of the test specimen[36,41].

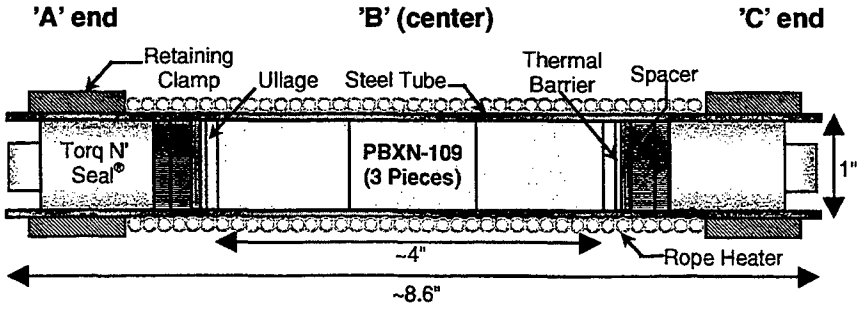

Figure 46. Modified Small-scale Slow Cookoff Pipe Specimen[36]

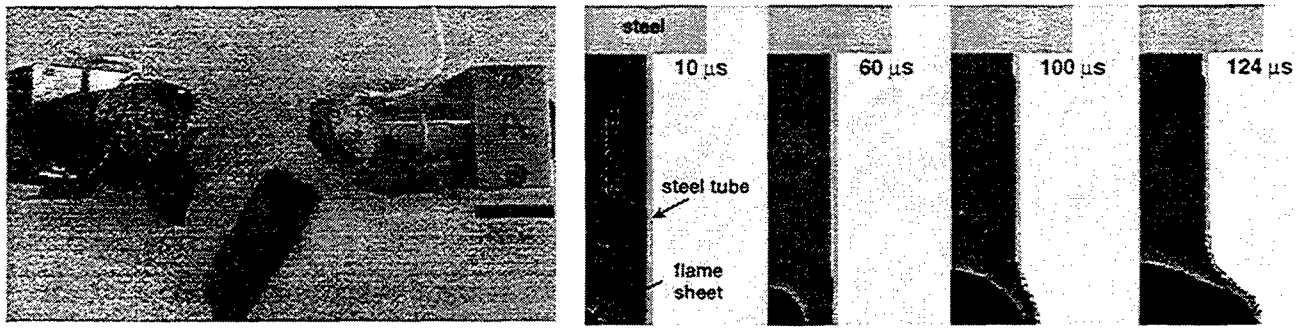

Figure 47. Post Test Debris[41] and Calculated Reaction Front Propagation and Pipe Expansion/Deformation[36] Indicating a Pressure Failure in the Center of the Specimen

Although more work is required to improve and adapt these computational methods to capture the complete physics of solid rocket motor cookoff, the modeling techniques developed in recent years provide an excellent foundation for further enhancement. Slow cookoff model development and validation efforts are continuing at DoD and DOE laboratories, and could possibly be leveraged to address fast cookoff modeling as well. Detailed characterization of liner pyrolysis and case-liner debond formation has not been included in the advanced finite element/finite difference models demonstrated above. Instead, the models predict heat transfer and ignition based on case/propellant properties and propellant chemical reaction/decomposition. Incorporation of liner physical behavior into a finite element/difference framework should be straightforward however.

The coupled modeling approach might be used in conjunction with a well-instrumented subscale test protocol to estimate the response of a much larger motor in the bonfire test. The key is to calibrate a model of the system in question by demonstrating accurate modeling of the failure mode as observed in the subscale test representative of the interaction between the motor design and the fire environment (assuming of course that the model approach has been validated), and then exercise the model applying boundary conditions (thermal input parameters, etc.) appropriate to a larger scale test, possibly using parametric sensitivity analysis to examine scaling results. Thus, further model development and validation efforts are warranted.

5.0 FAST COOKOFF TESTING RESULTS WITH HIGH ENERGY (SMALL CRITICAL DIAMETER) PROPELLANTS

The final section of this report summarizes findings of fast cookoff parametric test programs and other miscellaneous full-scale test results with solid rocket motors containing high-energy propellants. The purpose of this section is to examine the effect (if any) of propellant shock sensitivity and detonation properties on hazard response to credible accident scenarios. A large amount of fast cookoff test data for rocket motors has been collected during the U.S. Navy insensitive munitions (IM) program and precursor programs. Other services have reported some relevant motor fast cookoff data, but to a much more limited extent.

The U.S. Navy conducted an interesting full-scale parametric test series using three 8-inch diameter Shrike/Sparrow motor cases and three classes of solid propellant formulations. The objective was to develop baseline data on rocket motor responses to various hazard stimuli as part of the Insensitive Munitions Advanced Development (IMAD) program[5,42]. Motor case types included conventional steel, steel strip laminate, and filament wound fiber/epoxy composite. The standard test item (steel motor case) is shown in Fig. 48. Motors were loaded in standard five-point star grain configuration with three propellant types: standard Al/AP-based; non-aluminized AP-based reduced smoke; and high performance aluminized AP-based propellant containing HMX. The high performance propellant formulation contained about 14% HMX. A similar (and possibly the same) propellant has a reported critical diameter of between 2-3 inches[43]. Tests with all three motor case types and high performance HMX containing propellant were judged to result in mild burning responses as defined in MIL-STD 2105A[42].

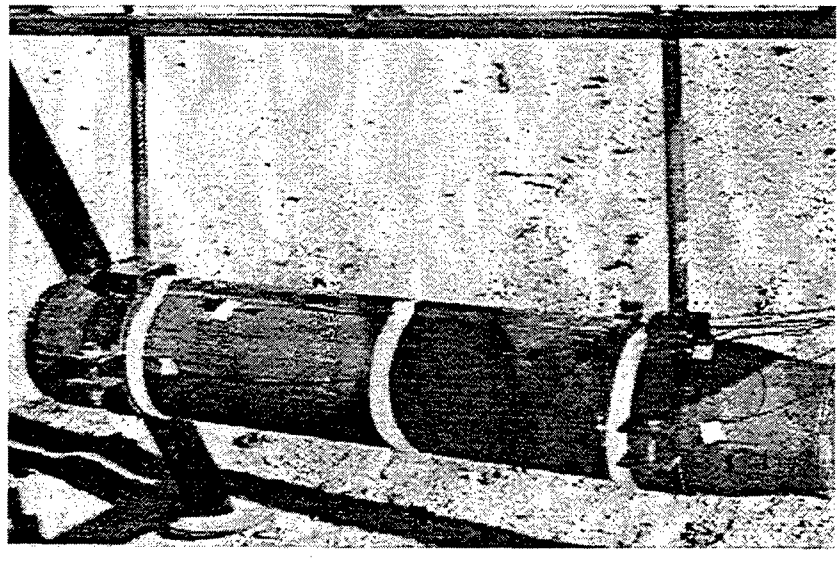

Figure 48. 8-inch Diameter Shrike/Sparrow Steel Motor Case[42]. See also Fig. 3.

Leining et al[4] reported on tests for a highly detonable minimum smoke propellant formulation loaded in a five point star configuration in a similar Sparrow motor case[44]. The propellant has a measured critical diameter of about 0.25 inches[4]. This work was specifically performed to examine realistic hazard differences between conventional Class 1.3 and high-energy Class 1.1 propellants for air-launched missiles. The result was compared to an earlier Navy baseline test conducted on an operational Shrike missile (all-up-round) loaded with aluminized ammonium perchlorate based propellant. Both tests were reported as explosion responses. Note, however, that several Shrike motor-only (not AUR) tests have typically resulted in propulsion or deflagration reactions[45], so it appears that the presence of additional airframe structure may contribute to a more violent response. This is consistent with observed results from Farmer et al[5] with similar aluminized AP-based propellants in similar Shrike/Sparrow motor cases. On the other hand, Thacher[46] pointed out that another possible explanation for the explosion response was that the flame temperature of the fire rose slowly in this test, such that a time correction per MIL-STD 1648 was applied (suggesting that the motor

case was not weakened as much as it typically might have been at the time of propellant ignition). Furthermore, the complete configuration in the minimum smoke motor test (AUR or motor-only) was not reported. Finally, the internal motor case-liner used with the minimum smoke propellant was developed for the AP/polybutadiene Sparrow propellant; it is not known if any incompatibilities exist between the propellant and liner, but this could possibly affect the ultimate hazard response. These issues may cloud the assessment of results. In any case, no evidence of detonation (full or partial) was presented in the test summary with the minimum smoke propellant, and ultimately, Leining et al[4] concluded that introduction of Class 1.1 propellants would not affect the hazard severity of motor response in a fire scenario in the absence of warheads or other explosive donors.

Further evidence that high energy/small critical diameter propellants do not cause an increase in fast cookoff hazard response was provided in Navy parametric tests using a 13.5-inch diameter (shortened analog) Standard Missile motor configuration[47]. The test item is illustrated in Fig. 49. Two propellants were tested in a conventional steel cased motor configuration to allow direct comparison: a Class 1.1 minimum smoke propellant containing high levels of HMX and nitrate ester plasticizers; and the same Class 1.3 high performance aluminized AP-based propellant containing 14% HMX discussed previously (critical diameter of between 2-3 inches). While the critical diameter of the particular minimum smoke propellant has not been reported, it is reasonable to assume the critical diameter to be in the same range as other similar formulations - on the order of 0.25 inches. Results for both of these formulations were mild: propulsive and deflagration in two tests with the minimum smoke propellant; and burning and deflagration in two tests with the HMX-containing propellant, as defined in accordance with MIL-STD 1648. Again, the investigators concluded that introduction of Class 1.1 propellants does not increase the expected hazard severity of a motor in a fire scenario.

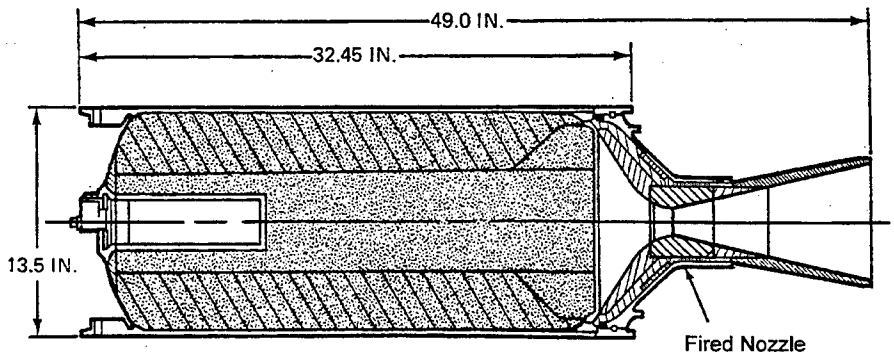

Figure 49. Shortened 13.5-inch Diameter Standard Missile Analog Motor[47].

Resistance to detonation of a Class 1.1 minimum smoke propellant rocket motor in fast cookoff was also reported by Panella[48]. The motor contained about 20 pounds of highly detonable propellant loaded in 7-inch diameter aluminum motor case (Fig. 50). The motor and all-up-round with warhead both responded in a mild burning fashion.

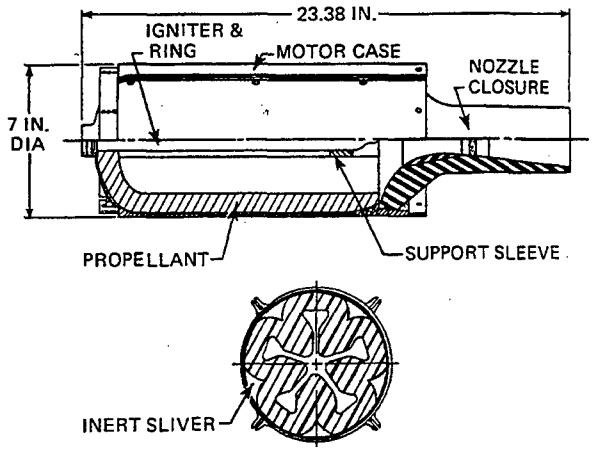

Figure 50. Schematic of Minimum Smoke Rocket Motor [48]

Thacher[46] also provides an interesting example of nondetonability of a large strategic class rocket motor loaded with Class 1.1 propellant in a fast cookoff scenario. An external view of the motor tested is shown in Fig. 51. The motor has a filament wound composite motor case loaded with a composite modified double base propellant (including nitramines). The critical diameter of the propellant has not been identified; however, similar formulations have been reported to have a critical diameter of 0.5 inches or less[49]. Results included intermittent propellant chuffing burning following a mild case burst. The mild response is not surprising, however, due to enhanced venting (deterioration of the confining structure) with the composite case construction used in this motor[50].

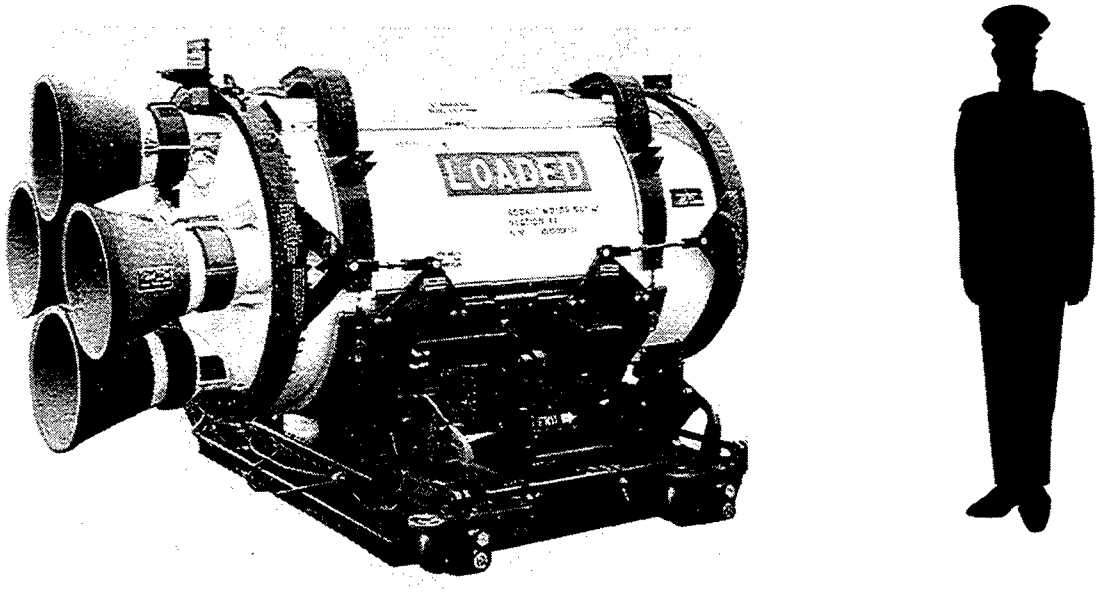

Figure 51. Class 1.1 Strategic Missile Rocket Motor[51]

6.0 SUMMARY

A significant amount of research, development, test, and evaluation work related to the fast cookoff hazard response of solid rocket motors has been conducted over the last 30 years. This work has advanced the fundamental understanding of SRM failure modes occurring under fast cookoff conditions, thereby establishing a technical foundation for development of subscale analog and/or modeling approaches to predict the fast cookoff response of full-scale motors. This report consolidates pertinent RDT&E work in a single source, with the goal of assisting the technical and safety communities in identifying further research necessary to complete the development and validation of a subscale testing and/or modeling protocol for fast cookoff assessment of solid rocket motors.

7.0 ACKNOWLEDGEMENTS

The author wishes to express his appreciation to the following individuals for their technical review of this report:

Dr. Jon Maienschein, Lawrence Livermore National Laboratory, Livermore, CA
Mr. Andy Victor, Victor Technology, San Ramon, CA

8.0 REFERENCES

[1] Vetter, R. F., *Reduction of Fuel Fire Cook-off Hazard of Rocket Motors*, Naval Weapons Center, China Lake, CA, NWC TP 5921 (1977), U-A.

[2] Clark, D. P., Harper, M. R., Munson, W. O., Pratt, D. A., Taylor, R. D., and Watkins, C. R., *Missile Propellant Safety Evaluation - Task II Report*, Morton Thiokol, Inc., Brigham City, UT, AFAL TR-87-003 (1987a), U-C.

[3] Clark, D. P., Munson, W. O., Taylor, R. D., Pratt, D. A., McDermott, S. M., Harper, M. R., and Werthmann, K. J., *Missile Propellant Safety Evaluation - Task III Report*, Morton Thiokol, Inc., Brigham City, UT, AFAL TR-87-003 (1987b), U-C.

[4] Leining, R. B., Thacher, J. H., Brown, B., Christensen, L. W., Clifford, R. A., Currit, D. H., Isom, K. B., Keefe, R. L., Peterson, R. L., and Thomas, K. D., *Air-Launched Missile Motor Behavior*, Hercules, Inc., Magna, UT, AFRPL-TR-81-45 (1981), U-B. See also Hannum, J. A. E. (ed), *Second AFRPL/NWC Workshop on Air Launched Missile Motor Behavior*, Chemical Propulsion Information Agency, Laurel, MD, CPIA Publication 337 (1981), U-B.

[5] Farmer, J. W., Pritchard, R. W., and Davis, L. M., *A Study of Rocket Motors and Large-Scale Hazards Testing for the Insensitive Munitions Advanced Development (IMAD) Propulsion Program*, Naval Weapons Center, China Lake, CA, NWC TP 6840 (1988), U-C. Includes a supplemental videotape of selected test records, "IMAD Propulsion – Large Scale Hazards Testing," V.P. No. 88-187.

[6] Rogerson, D. J., "Internal Observation of Rocket Motor Open Pool Fast Cook-offs Using High Energy Realtime Radiography," Naval Weapons Center, China Lake, CA, in *Proc. JANNAF Propulsion Systems Hazards Subcommittee Meeting*, 28-30 March 1988, CPIA Publication 477 Volume I, pp. 167-174 (1988), U-A.

[7] Hicks, T. A., "Structural Aspects of Rocket Motor Cookoff," Naval Weapons Center, China Lake, CA, in *Proc. JANNAF Propulsion Systems Hazards Subcommittee Meeting*, 29-31 October 1980, CPIA Publication 330 Volume II, pp. 231-250 (1980), U-B.

[8] Vetter, R. F., "Concepts for Improving Safety of Fuel Fire Envelopment Reaction of Solid Rocket Motors," Naval Weapons Center, China Lake, CA, in *Proc. JANNAF Propulsion Meeting*, 14-17 February 1983, CPIA Publication 370 Volume IV, pp. 243-249 (1983), U-B.

[9] Vernon, G. A., "Small-Scale Simulation of Motor Liner Behavior," Naval Weapons Center, China Lake, CA, in *Proc. JANNAF Propulsion Systems Hazards Subcommittee Meeting*, 29-31 October 1980, CPIA Publication 330 Volume II, pp. 293-310 (1980), U-B.

[10] Fung, M. L., Casper, T., Hicks, T., and Vetter R., *Thermal Modeling of Insulator/Liner*, Naval Weapons Center, China Lake, CA, NWC TP 6336 (1982), U-B.

[11] Roark, R. J., *Formulas for Stress and Strain*, McGraw-Hill Book Company, Inc. (1954).

[12] Victor, A. C., "Exploring Cookoff Mysteries," Victor Technology, Ridgecrest, CA, in *Proc. JANNAF Propulsion Systems Hazards Subcommittee Meeting*, 1-4 August 1994, CPIA Publication 615, pp. 177-198 (1994), U-A.

[13] Fontenot, J. S., "Status of DoD Cookoff Methodology Development," Naval Air Warfare Center, China Lake, CA, in *Proc. JANNAF Propulsion Meeting*, 24-27 February 1992, CPIA Publication 580 Volume II, pp. 343-345 (1992), U-D.

[14] Cost, T. L., "Thermal Protection of Munitions by Canisters in Fuel Fire Environments," Athena Engineering Company, Huntsville, AL, in *Proc. JANNAF Propulsion Systems Hazards Subcommittee Meeting*, 1-4 August 1994, CPIA Publication 615, pp. 259-271 (1994), U-C.

[15] Thomas, W. B., Vance, S. L., Jones, D. J., and Cost, T. L., "Fast Cookoff Testing and Analysis for the Army IM Database," Thiokol Corporation, Huntsville, AL, in *Proc. JANNAF Propulsion Systems Hazards Subcommittee Meeting*, 27 April-1 May 1992, CPIA Publication 582 Volume I, pp. 489-496 (1992), U-C.

[16] Thacher, J. H., Wetherell, R. B., and Anderson, J. M., "(DELETED) Motor Detonation Studies: An Overview," Hercules Inc., Magna, UT, in *Proc. 15th JANNAF Combustion Meeting*, CPIA Publication 297 Volume III, pp. 7-34 (1979), U-B.

[17] Isom, K. B., Keefe, R. L., and Thacher, J. H., "Standardized Propellant Testing for DDT Potential," Hercules, Incorporated, Magna, UT, in *Proc. 15th JANNAF Combustion Meeting*, CPIA Publication 297 Volume III, pp. 169-194 (1979), C.

[18] Price, C. F., Boggs, T. L., Gould, R. A., Eisel, J. L., and Zurn, D. E., "CBRED II Program as Used with Closed Bomb Testing of Damaged Propellant from LAM and Shotgun Tests," Naval Weapons Center, China Lake, CA, in *Proc. 15th JANNAF Combustion Meeting*, CPIA Publication 297 Volume III, pp. 149-167 (1979), C.

[19] Hodson, G. B., "Propellant Fragmentation in 30-inch Test Motor 3SF-52," Hercules, Inc., Magna, UT, in *Proc. JANNAF Propulsion Systems Hazards Subcommittee Meeting*, 29-31 October 1980, CPIA Publication 330 Volume II, pp. 317-346 (1980), C.

[20] Knaur, J. A., "Technical Investigation of 11 January 1985 Pershing II Motor Fire," U.S. Army Missile Command, Redstone Arsenal, AL, in *Minutes of the 22nd DDESB Explosives Safety Seminar*, Volume I, pp. 1005-1013 (26-28 August 1986), U-A.

[21] Stephens, W. D., *Technical Investigation of 11 January 1985 Pershing II Motor Fire*, U.S. Army Missile Command, Redstone Arsenal, AL, TR RK-85-9, Volume I (pp. 76-85) and Volume IIID, pp. 931-965; pp. 1003-1007 (1985), U-X.

[22] Stephens, W. D., "Hardware as Evidence in an Accident Investigation," U.S. Army Missile Command, Redstone Arsenal, AL, in *Proc. JANNAF Propulsion Meeting*, 26-28 August 1986, CPIA Publication 455 Volume I, pp.1-5 (1986), U-A.

[23] Tarver, C. M., Tao, W. C. and Lee, C. G., "Sideways Plate Push Test for Detonating Solid Explosives," Lawrence Livermore National Laboratory, Livermore, CA, *Propellants, Explosives, Pyrotechnics*, **21**, 238-246 (1996).

[24] Baker, E. L. and Stiel, L. I., "Improved Quantitative Explosive Performance Prediction Using Jaguar," U.S. Army Tank-automotive and Armaments Command, Armament Research, Development, and Engineering Center, Picatinny Arsenal, NJ, in *Proc. NDIA Insensitive Munitions & Energetic Materials Technology Symposium* (6-9 October 1997), U-A.

[25] Miller, P. J. and Woody, D. L., "Reaction Kinetics of Aluminum Particles in Detonation Gases," Naval Surface Warfare Center, Indian Head, MD, in *Proc. JANNAF Propulsion Systems Hazards Subcommittee Meeting*, 1-4 August 1994, CPIA Publication 615, pp. 413-419 (1994), U-C.

[26] Maienschein, J. L., Lee, E. L., Reaugh, J. E., Merrill, C. I., and Lambert, R. R., *Modeling the Impact Response of Booster Propellants*, Lawrence Livermore National Laboratory, Livermore, CA, in *Proc. JANNAF Propulsion Systems Hazards Subcommittee Meeting*, 27-30 October 1997, CPIA Publication 657 Volume 2, pp. 163-177 (1997), U-C.

[27] Merrill, C., Lambert, R., Maienschein, J., Nichols, A., Lee, E., and Tao, W., "Booster Propellant Explosive Behavior with Composition Changes," in *Proc. JANNAF Propulsion Systems Hazards Subcommittee Meeting*, 23-27 October 1995, CPIA Publication 628, pp. 353-372 (1995), U-C.

[28] Raun, R. L., Butcher, A. G., Caldwell, D. J., and Beckstead, M. W., "An Approach for Predicting Cookoff reaction Time and Reaction Severity," Hercules, Inc., Magna, UT, in *Proc. JANNAF Propulsion Systems Hazards Subcommittee Meeting*, 27 April – 1 May 1992, CPIA Publication 582 Volume I, pp. 497-504 (1992), U-C.

[29] Atwood, A. I., Curran, P. O., Kraeutle, K. J., Heimdahl, O. E. R., Hanson-Parr, D. M., Parr, T. P., and Johns, H. J., "A Slow Cookoff Methodology Study," Naval Air Warfare Center, China Lake, CA, in *Proc. 18th JANNAF Propulsion Systems Hazards Subcommittee Meeting*, 18-21 October 1999, CPIA Publication 690 Volume I, pp. 133-147 (1999), U-A.

[30] Schmitt, R. G., Erikson, W. W., Atwood, A. I., and Johns, H., "Analysis of the NAWC Validation Cookoff Test," Sandia National Laboratories, Albuquerque, NM, in *Proc. 18th JANNAF Propulsion Systems Hazards Subcommittee Meeting*, 18-21 October 1999, CPIA Publication 690 Volume II, pp. 23-34 (1999), U-C.

[31] Renlund, A. M., Kaneshige, M. J., Schmitt, R. G., and Wellman, G. W., "Mechanical Response and Decomposition of Thermally Degraded Energetic Materials: Experiments and Model Simulations," Sandia National Laboratories, Albuquerque, NM, in *Proc. 18th JANNAF Propulsion Systems Hazards Subcommittee Meeting*, 18-21 October 1999, CPIA Publication 690 Volume I, pp. 43-49 (1999), U-A.

[32] Schmitt, R. G., Wellman, G. W., Renlund, A. M., and Miller, J. C., "A Constitutive Model for Confined HMX During Cookoff," Sandia National Laboratories, Albuquerque, NM, in *Proc. 17th JANNAF Propulsion Systems Hazards Subcommittee Meeting*, 7-11 December 1998, CPIA Publication 681 Volume I, pp. 95-104 (1998), U-A.

[33] Compton, W. R., "Violence of Reaction Analysis for JSOW/BLU-108 in a Fast Cookoff Environment," Dcompton & Associates, Ridgecrest, CA, in *Proc. JANNAF 17th Propulsion Systems Hazards Subcommittee Meeting*, 7-11 December 1998, CPIA Publication 681 Volume II, pp. 41-52 (1998) U-C.

[34] Mader, C. L., *Numerical Modeling of Detonations*, Univ. of California Press, Berkeley, California, pp. 316-320 (1979).

[35] Cheret, R., *Detonation of Condensed Explosives*, Springer-Verlag, New York, pp. 182-186 (1993).

[36] Erikson, W. W., Schmitt, R. G., Atwood, A. I., and Curran, P. D., "Coupled Thermal-Chemical-Mechanical Modeling of Validation Cookoff Experiments," Sandia National Laboratories, Albuquerque, NM, in *Proc. JANNAF 19th Propulsion Systems Hazards Subcommittee Meeting*, 13-17 November 2000, CPIA Publication 704 Volume II, pp. 53-66 (2000), U-B.

[37] Baer, M. R., Kipp, M. E., Schmitt, R. G., and Hobbs, M. L., "Towards Assessing the Violence of Reaction During Cookoff of Confined Energetic Materials," Sandia National Laboratories, Albuquerque, NM, in *Proc. JANNAF Propulsion Systems Hazards Subcommittee Meeting*, 4-8 November 1996, CPIA Publication 645 Volume I, pp. 249-257 (1996), U-A.

[38] Schmitt, R. G. and Baer, T. A., "Millisecond Burning of Confined Energetic Materials During Cookoff," in *Proc. JANNAF Propulsion Systems Hazards Subcommittee Meeting*, 27-30 October 1997, CPIA Publication 657 Volume I, pp. 61-71 (1997), U-A.

[39] McClelland, M. A., Tran, T. D., Cunningham, B. J., Weese, R. K., and Maienschein, J. L., "Cookoff Response of PBXN-109: Material Characterization and ALE3D Model," Lawrence Livermore National Laboratory, Livermore, CA, in *Proc. JANNAF 19th Propulsion Systems Hazards Subcommittee Meeting*, 13-17 November 2000, CPIA Publication 704 Volume I, pp. 191-203 (2000), U-A.

[40] Nichols, A. L., Couch, R., Maltby, J. D., McCallen, R. C., Otero, I., and Sharp, R., "Coupled Thermal/Chemical/Mechanical Modeling of Energetic Materials in ALE3D," Lawrence Livermore National Laboratory, Livermore, CA, in *Proc. JANNAF Propulsion Systems Hazards Subcommittee Meeting*, 4-8 November 1996, CPIA Publication 645 Volume I, pp. 239-248 (1996), U-A.

[41] Atwood, A. I., Curran, P. O., Decker, M. W., Boggs, T. L., and Erikson, W. W., "Experiments for Cookoff Model Validation, Naval Air Warfare Center," China Lake, CA, in *Proc. JANNAF 19th Propulsion Systems Hazards Subcommittee Meeting*, 13-17 November 2000, CPIA Publication 704 Volume I, pp. 205-220 (2000), U-A.

[42] Stanley, G., *Rocket Motor Large Scale Hazards Testing for the Insensitive Munitions Advanced Development Propulsion Program*, Comarco, Inc., China Lake, CA, NWC TP 7086 (1991), U-C.

[43] Richter, H. P., "Critical Diameter/Detonability Studies of Composite Propellant," in *Minutes of the 2-3 June 1992 Meeting of the JANNAF Propulsion Systems Hazards Subcommittee Safety & Hazard Classification Panel*, PSHS-WBT-JEC/CTH-10-92 (1992), U.

[44] Silva, A. M., Scott, D. E., and Herriott, G. E., *Minimum Smoke Motor Demonstration Program*, Hercules, Inc., Cumberland, MD, AFRPL-TR-80-54 (1980) U-B.

[45] *Insensitive Munitions Characteristics of Air-launched In-service Weapons – Summary Report of Fast Cookoff Times, Reactions, and Hazards of Bombs, Rockets, Aircraft Guns, Air-launched Missiles, Mines, and Torpedos*, Naval Air Warfare Center, NAWCWPNS TP 8022 (1992), U-C.

[46] Thacher, J. H., *Explosive Hazards of Air-Launched Propulsion Systems*, Hercules Inc., Magna, UT, AFRPL-TR-77-9 (1977), U-B.

[47] Feist, R. W. and East, J. L., "Sensitivity Testing of Class 1.1 and Class 1.3 Propellants, Naval Weapons Center," China Lake, CA, in *Proc. JANNAF Propulsion Meeting*, 9-12 April 1985, CPIA Publication 425 Volume III, pp. 111-116 (1985), U-D.

[48] Panella, E. A., "Slow and Fast Cookoff Tests of the (DELETED) Missile," Naval Weapons Center, China Lake, CA, in *Proc. JANNAF Propulsion Meeting*, 9-12 April 1985, CPIA Publication 425 Volume III, pp. 233-237 (1985), U-D.

[49] Jaffe, I. and Roberson, E., *The Critical Diameter and Detonation Velocity of Double Base Propellants*, Naval Ordnance Laboratory, White Oak, MD, NOLTR 65-112 (1965), U.

[50] Cocchiaro, J. E., *Solid Rocket Motor Components for Insensitive Munitions*, Chemical Propulsion Information Agency, Columbia, MD, CPTR 93-53 (1993), U-D.

[51] Moore, T. L. (ed.), *CPIA/M1 Rocket Motor Manual*, Volume I, Unit 413 (1964), U.

INITIAL DISTRIBUTION

- ARMY -

ARMY AVIATION AND MISSILE COMD/REDSTONE ARSENAL
- 1 BEN F. WILSON
- 1 DOCUMENTS, AMSMI-RD-CS-R
- 1 DR. JAMES G. CARVER
- 1 DR. WILLIAM MELVIN
- 1 MR. J. MICHAEL LYON
- 1 TERRY L. VANDIVER

ARMY RESEARCH LAB/ABERDEEN
- 1 LOUISE LETENDRE

ARMY RSCH OFC/RESEARCH TRIANGLE PARK
- 1 D. M. MANN

ARMY TANK AUTOMOTIVE & ARMAMENT COMD/PICATINNY
- 1 PATRICIA AYS

- NAVY -

NAVAL AIR WARFARE CTR/CHINA LAKE
- 1 CHRIS TOFTNER
- 1 DR. FRED S. BLOMSHIELD
- 1 DR. GEOFFREY A. LINDSAY
- 1 DR. JAMES HOOVER
- 1 DR. MAY L. CHAN
- 1 DR. RUSSELL REED
- 1 HERB RICHTER
- 1 HOWARD BOWMAN
- 1 JACK M. PAKULAK
- 1 JAMES A. GROSS
- 1 JAMES A. LOUNDAGIN
- 1 JAMES C. BALDWIN
- 1 MARY S. PAKULAK
- 1 STUART R. BLASHILL
- 1 TECH LIB/P. BACKES
- 1 THOMAS L. BOGGS

NAVAL SURFACE WARFARE CTR/INDIAN HEAD
- 1 MICHAEL P. SIKORA

- AIR FORCE -

AFRL/EDWARDS AFB
- 1 DR. LAWRENCE P. QUINN
- 1 JOHN H. CLARK
- 1 LUCIANO SEDILLO
- 1 ROBERT C. CORLEY
- 1 TED MILES

AFRL/WPAFB
- 1 W. LEE BAIN

NATL AIR INTEL CTR/WPAFB
- 1 BEVERLY BRINK

- NASA -

NASA AEROSPACE INFO CTR/HANOVER
- 1 ACQUISITIONS DEPT

NASA GLENN RSCH CTR/CLEVELAND
- 1 SCOTT MEYER, MC 86-18
- 1 WOODROW WHITLOW

NASA JOHNSON SPACE CTR/HOUSTON
- 1 BARRY WITTSCHEN
- 1 GERALD SANDERS

NASA JSC WSTF/LAS CRUCES
- 1 LURLENE FORD/ET.AL.

NASA LANGLEY/HAMPTON
- 1 MR. MELVIN LUCY
- 1 S. MILLER/MS-185 TECH LIB

NASA/MARSHALL SPACE FLIGHT CTR
- 1 CN22/LIBRARY
- 1 DR. TERRY F. GREENWOOD

NASA/WASHINGTON, DC
- 1 DAVID STONE
- 1 W. R. FRAZIER, CODE QS

- OTHER GOV'T. -

DEF TECH INFO CTR/FT BELVOIR
- 2 DTIC-OCC

DTRA/ARLINGTON
- 1 FRANK TRACESKI

- NON-GOV'T. -

AEROJET/SACRAMENTO
- 1 AEROJET-TIC

AEROSPACE/LOS ANGELES
- 1 BENITA CAMPBELL, M1-199

ALLIANT AEROSPACE COMPANY/MAGNA
- 1 LIBRARY, M/S H

ALLIANT MISSILE PRODUCTS COMPANY LLC/ROCKET
- 1 DOTTIE LYON

ATLANTIC RESEARCH CORP/GAINESVILLE
- 1 TECHNICAL INF CTR

BOEING COMPANY/CANOGA PARK
- 1 H. E. SNELL, TIC BA29

BOEING/SEATTLE
- 1 LIB ACQ

LLNL/LIVERMORE
- 1 BETTE MOORE

PACIFIC SCIENTIFIC ENERGETIC MATERIALS CO/CHANDLER
- 1 SMALLWOOD/KORCSMAROS

PENNSYLVANIA STATE UNIV/STATE COLLEGE
- 1 DR. DANIEL KIELY

PRIMEX AEROSPACE COMPANY/REDMOND
- 1 JAMES GURLEY

RAYTHEON COMPANY/TUCSON
- 1 SHANNON MACK

SANDIA NATIONAL LABS/ALBUQUERQUE
- 1 M. GRUBELICH
- 1 S. LANDENBERGER

TALLEY/MESA
- 1 SECURITY OFFICE

THIOKOL PROPULSION/ELKTON
- 1 THOMAS HOLMAN

THIOKOL/BRIGHAM CITY
- 1 ELLEN WAGSTAFF

UNITED TECHNOLOGIES/SAN JOSE
- 1 TECHNICAL LIBRARY

UNIVERSAL PROPULSION COMPANY INC/PHOENIX
- 1 JAMES J. BAKER

CHEMICAL PROPULSION INFORMATION AGENCY

THE JOHNS HOPKINS UNIVERSITY, Whiting School of Engineering
10630 Little Patuxent Parkway, Suite 202, Columbia, MD 21044-3204
Telephone: (410) 992-7300 • Telefax: (410) 730-4969 • e-mail: cpia@jhu.edu • www.cpia.jhu.edu

4 September 2001

MEMORANDUM

TO: Distribution

SUBJECT: ***Errata*** for CPIA Chemical Propulsion Technology Review, CPTR 72 *Subscale Fast Cookoff Testing and Modeling for the Hazard Assessment of Large Rocket Motors*

The enclosed corrected page 18 should be inserted/attached to your copy of CPTR 72. The original document contained clerical errors to Figures 21 and 22. We apologize for any inconvenience that this error may have presented to the user.

James E. Cocchiaro
(410) 992-9950 X208
james.cocchiaro@cpia.jhu.edu

Distribution: see attached

INITIAL DISTRIBUTION

- ARMY -

ARMY AVIATION AND MISSILE COMD/REDSTONE ARSENAL
- 1 BEN F. WILSON
- 1 DOCUMENTS, AMSMI-RD-CS-R
- 1 DR. JAMES G. CARVER
- 1 DR. WILLIAM MELVIN
- 1 MR. J. MICHAEL LYON
- 1 TERRY L. VANDIVER

ARMY RESEARCH LAB/ABERDEEN
- 1 LOUISE LETENDRE

ARMY RSCH OFC/RESEARCH TRIANGLE PARK
- 1 D. M. MANN

ARMY TANK AUTOMOTIVE & ARMAMENT COMD/PICATINNY
- 1 PATRICIA AYS

- NAVY -

NAVAL AIR WARFARE CTR/CHINA LAKE
- 1 CHRIS TOFTNER
- 1 DR. FRED S. BLOMSHIELD
- 1 DR. GEOFFREY A. LINDSAY
- 1 DR. JAMES HOOVER
- 1 DR. MAY L. CHAN
- 1 DR. RUSSELL REED
- 1 HERB RICHTER
- 1 HOWARD BOWMAN
- 1 JACK M. PAKULAK
- 1 JAMES A. GROSS
- 1 JAMES A. LOUNDAGIN
- 1 JAMES C. BALDWIN
- 1 MARY S. PAKULAK
- 1 STUART R. BLASHILL
- 1 TECH LIB/P. BACKES
- 1 THOMAS L. BOGGS

NAVAL SURFACE WARFARE CTR/INDIAN HEAD
- 1 MICHAEL P. SIKORA

- AIR FORCE -

AFRL/EDWARDS AFB
- 1 DR. LAWRENCE P. QUINN
- 1 JOHN H. CLARK
- 1 LUCIANO SEDILLO
- 1 ROBERT C. CORLEY
- 1 TED MILES

AFRL/WPAFB
- 1 W. LEE BAIN

NATL AIR INTEL CTR/WPAFB
- 1 BEVERLY BRINK

- NASA -

NASA AEROSPACE INFO CTR/HANOVER
- 1 ACQUISITIONS DEPT

NASA GLENN RSCH CTR/CLEVELAND
- 1 SCOTT MEYER, MC 86-18
- 1 WOODROW WHITLOW

NASA JOHNSON SPACE CTR/HOUSTON
- 1 BARRY WITTSCHEN
- 1 GERALD SANDERS

NASA JSC WSTF/LAS CRUCES
- 1 LURLENE FORD/ET.AL.

NASA LANGLEY/HAMPTON
- 1 MR. MELVIN LUCY
- 1 S. MILLER/MS-185 TECH LIB

NASA/MARSHALL SPACE FLIGHT CTR
- 1 CN22/LIBRARY
- 1 DR. TERRY F. GREENWOOD

NASA/WASHINGTON, DC
- 1 DAVID STONE
- 1 W. R. FRAZIER, CODE QS

- OTHER GOV'T. –

DEF TECH INFO CTR/FT BELVOIR
- 2 DTIC-OCC

DTRA/ARLINGTON
- 1 FRANK TRACESKI

- NON-GOV'T. -

AEROJET/SACRAMENTO
- 1 AEROJET-TIC

AEROSPACE/LOS ANGELES
- 1 BENITA CAMPBELL, M1-199

ALLIANT AEROSPACE COMPANY/MAGNA
- 1 LIBRARY, M/S H

ALLIANT MISSILE PRODUCTS COMPANY LLC/ROCKET
- 1 DOTTIE LYON

ATLANTIC RESEARCH CORP/GAINESVILLE
- 1 TECHNICAL INF CTR

BOEING COMPANY/CANOGA PARK
- 1 H. E. SNELL, TIC BA29

BOEING/SEATTLE
- 1 LIB ACQ

LLNL/LIVERMORE
- 1 BETTE MOORE

PACIFIC SCIENTIFIC ENERGETIC MATERIALS CO/CHANDLER
- 1 SMALLWOOD/KORCSMAROS

PENNSYLVANIA STATE UNIV/STATE COLLEGE
- 1 DR. DANIEL KIELY

PRIMEX AEROSPACE COMPANY/REDMOND
- 1 JAMES GURLEY

RAYTHEON COMPANY/TUCSON
- 1 SHANNON MACK

SANDIA NATIONAL LABS/ALBUQUERQUE
- 1 M. GRUBELICH
- 1 S. LANDENBERGER

TALLEY/MESA
- 1 SECURITY OFFICE

THIOKOL PROPULSION/ELKTON
- 1 THOMAS HOLMAN

THIOKOL/BRIGHAM CITY
- 1 ELLEN WAGSTAFF

UNITED TECHNOLOGIES/SAN JOSE
- 1 TECHNICAL LIBRARY

UNIVERSAL PROPULSION COMPANY INC/PHOENIX
- 1 JAMES J. BAKER